Naval Research Laboratory

Washington, DC 20375-5320

NRL/MR/6110--11-9330

Beaufort Sea Methane Hydrate Exploration: Energy and Climate Change

R.B. Coffin
L.J. Hamdan
J.P. Smith

Chemical Dynamics and Diagnostics Branch
Chemistry Division

R. Plummer
L. Millholland

SAIC
Washington, DC

R. Larson

St. Mary's College of Maryland
St. Mary's City, Maryland

W. Wood

Seafloor Sciences Branch
Marine Geosciences Division

May 27, 2011

REPORT DOCUMENTATION PAGE

Form Approved
OMB No. 0704-0188

1. REPORT DATE *(DD-MM-YYYY)*	**2. REPORT TYPE**	**3. DATES COVERED** *(From - To)*
27-05-2011	Memorandum	September 2009

4. TITLE AND SUBTITLE

Beaufort Sea Methane Hydrate Exploration: Energy and Climate Change

5a. CONTRACT NUMBER

5b. GRANT NUMBER

5c. PROGRAM ELEMENT NUMBER

6. AUTHOR(S)

R.B. Coffin, L.J. Hamdan, J.P. Smith, R. Plummer,* L. Millholland,*
R. Larson,† and W. Wood

5d. PROJECT NUMBER

5e. TASK NUMBER

5f. WORK UNIT NUMBER
61-5557-6-0-5

7. PERFORMING ORGANIZATION NAME(S) AND ADDRESS(ES)

Naval Research Laboratory
4555 Overlook Avenue, SW
Washington, DC 20375-5320

8. PERFORMING ORGANIZATION REPORT NUMBER

NRL/MR/6110--11-9330

9. SPONSORING / MONITORING AGENCY NAME(S) AND ADDRESS(ES)

Office of Naval Research
One Liberty Center, Code 33
875 North Randolph Street, Suite 1425
Arlington, VA 22203-1995

10. SPONSOR / MONITOR'S ACRONYM(S)

ONR

11. SPONSOR / MONITOR'S REPORT NUMBER(S)

12. DISTRIBUTION / AVAILABILITY STATEMENT

Approved for public release; distribution is unlimited.

13. SUPPLEMENTARY NOTES

*SAIC, c/o Naval Research Laboratory, 4555 Overlook Avenue, SW, Washington, DC 20375.
†St. Mary's College of Maryland, Department of Chemistry and Biochemistry, 18592 East Fisher Road, St. Mary's City, MD 20686.

14. ABSTRACT

This is a geochemical report for the MITAS 1 expedition on the Beaufort Sea during September 2009, aboard the USCG Polar Sea. The overall cruise focus integrated research expertise in coastal ocean geophysics, sediment geochemistry, dissolved and free methane fluxes through the water column and into the atmosphere, sediment and water column microbiology and biogeochemistry, and detailed characterization of the sub-seafloor geology to address the following research topics: 1) Acquire and integrate seismic, heatflow, geochemical, and lithostratigraphic data for evaluation of deep sediment hydrate distributions; 2) Estimate spatial variation and controls on the vertical methane diffusion as compared to variations in lithostratigraphy, geologic structures, water column temperatures, heatflow, seismic profiles, and water depth; 3) Develop and calibrate models to evaluate sediment hydrate loading, hydrate destabilization through warming, and the fate of methane after hydrate destabilization; 4) Determine and model the transport of methane from the sediment through the water column into the atmosphere; 5) Study the control of total methane emissions by microbial methane consumption in the sediment and in the water column; 6) Study the contribution of methane to the benthic and pelagic carbon cycling. This report provides a summary of onboard geochemical analyses of sediment porewater through the regions cored and supports data interpretation for the research topics listed above.

15. SUBJECT TERMS

Arctic | Energy | Geochemistry
Methane hydrate | Climate change

16. SECURITY CLASSIFICATION OF:			**17. LIMITATION OF ABSTRACT**	**18. NUMBER OF PAGES**	**19a. NAME OF RESPONSIBLE PERSON**
					Richard B. Coffin
a. REPORT	**b. ABSTRACT**	**c. THIS PAGE**	UL	34	**19b. TELEPHONE NUMBER** *(include area code)*
Unclassified	Unclassified	Unclassified			(202) 767-0065

Standard Form 298 (Rev. 8-98)
Prescribed by ANSI Std. Z39.18

Table of Contents **Page#**

Table of Figures

Table of Contents Continued **Page#**

Table of Tables

Table of Appendices

I. Objectives

This is a geochemical report for the MITAS 1 expedition on the Beaufort Sea during September 2009, aboard the USCG Polar Sea (Appendix 1). The overall cruise focus (Appendix 2) integrated research expertise in coastal ocean geophysics, sediment geochemistry, dissolved and free methane fluxes through the water column and into the atmosphere, sediment and water column microbiology and biogeochemistry, and detailed characterization of the sub-seafloor geology to address the research topics listed below.

- Acquire and integrate seismic, heatflow, geochemical, and lithostratigraphic data for evaluation of deep sediment hydrate distributions.
- Estimate spatial variation and controls on the vertical methane diffusion as compared to variations in lithostratigraphy, geologic structures, water column temperatures, heatflow, seismic profiles, and water depth.
- Develop and calibrate models to evaluate sediment hydrate loading, hydrate destabilization through warming, and the fate of methane after hydrate destabilization.
- Determine and model the transport of methane from the sediment through the water column into the atmosphere.
- Study the control of total methane emissions by microbial methane consumption in the sediment and in the water column.
- Study the contribution of methane to the benthic and pelagic carbon cycling.

This report provides a summary of onboard geochemical analyses of sediment porewater through the regions cored and supports data interpretation for the research topics listed above.

II. Introduction

Gas hydrate deposits, observed along continental margins and in Arctic tundra, contain a large quantity of methane (Kvenvolden, 1988, 1999). Recent studies estimate that the global volume of methane in marine sediments is between 500 and 2,500 Gt C (Milkov et al. 2003). The Arctic Ocean is only 1% of the total ocean volume, however, with an average ocean depth of 1361 meters, the continental slopes and rises contain thick sediment successions containing considerable organic-rich natural gas source deposits. Discrete high porosity and permeable lithologies result in high saturation gas hydrate accumulations (Max and Lowrie, 1993). In addition to potential coastal ocean hydrates, permafrost bearing and sub-permafrost hydrates in this region have developed in geological traps during the most recent glacial period when permafrost conditions resulted in lower temperature conditions in the near subsurface. Research on the East-Siberian and Laptev Sea show high fluxes of coastal methane to the water column and atmosphere with supersaturated methane concentrations range 2500% to 4400% (154 nM) interpreted to result from thermoabrasion of shallow hydrate beds resulting in gas releases (Shakhova et al., 2005). The Arctic Ocean is a key region for developing prediction and understanding of climate change and methane hydrate energy exploration.

Until recently, the general understanding for methane sourcing to the atmosphere has focused onshore in the Arctic tundra with a general assumption that the direct land-atmosphere interface is the dominant source (Gorham, 1991; Oechel et al., 1993; Frey and Smith, 2005). Recent research in the Arctic Ocean has initiated consideration of the methane contribution to greenhouse gases. Initial estimates for

Manuscript approved September 24, 2010.

increased vertical fluxes of methane in the Arctic Ocean originate from estimates of a rise in bottom water temperatures, causing sediment hydrate dissociation (Dickens et al., 1995), a lowered coastal ocean sea level (Paull et al. 1991) and the resulting undersea landslides (Rothwell et al., 1998). These studies initiated the "Clathrate Gun Hypothesis" (Kennett et al., 2002), which describes a late quaternary series of atmospheric warming events resulting in changes of the ocean circulation patterns and raised greenhouse gas concentrations. In an alternate view of ocean methane hydrate contribution to climate change δD analysis of Greenland ice cores suggested that the primary sources of methane during the Younger and Older Dryas periods were land based (Sowers, 2006). A more thorough evaluation of the distributions and concentrations of methane hydrates in Arctic permafrost and ocean will contribute to understanding of methane contribution to climate change.

The Mallik Wells, on the Mackenzie Delta, and the Mount Elber 01 well, on the North Slope of Alaska, demonstrates presence of high saturation gas hydrate accumulations in onshore, sub-permafrost reservoirs (Collet, 2003). These and other hydrate bearing formations extend offshore, thus an extensive distribution of hydrates through the submerged permafrost and coastal ocean is predicted. There have been large international efforts in both regions to evaluate the potential energy in the tundra deposits. Recent interest has also picked up for oil and hydrate exploration in the Beaufort and Chukchi Seas. A thorough evaluation of Arctic Ocean deep sediment hydrate distribution is needed to determine the potential for future energy.

III. Beaufort Sea Overview

The 476,000 sq km of the Beaufort Sea (Figure 1) extends to the northeast from Point Barrow, Alaska to the northeast of Prince Patrick Island, northward toward Banks Island and westward to the Chukchi Sea. The average depth of the Beaufort Sea is 1,004 m. The sediment character in this region is controlled by dispersal and re-suspension of river-borne sediments ice scouring, and coastal erosion and retreat (reviewed in Carmack and MacDonald, 2002). In the eastern Beaufort Sea, sediments deposited through the Holocene included terrestrial organic carbon concentrations from the Mackenzie River up to approximately130−160 tones/yr. In general, the shallow sediments are dominantly clay/silt with some sand and gravel from ice rafting in a few locations, overlain by a thin veneer of finer grained Holocene marine sediment. To the west of the Mackenzie River system, along the western Beaufort Shelf, sediment delivery results from numerous arctic river systems including the Colville River (Dunton et al. 2006). Our research focused on the stretch of Beaufort Sea

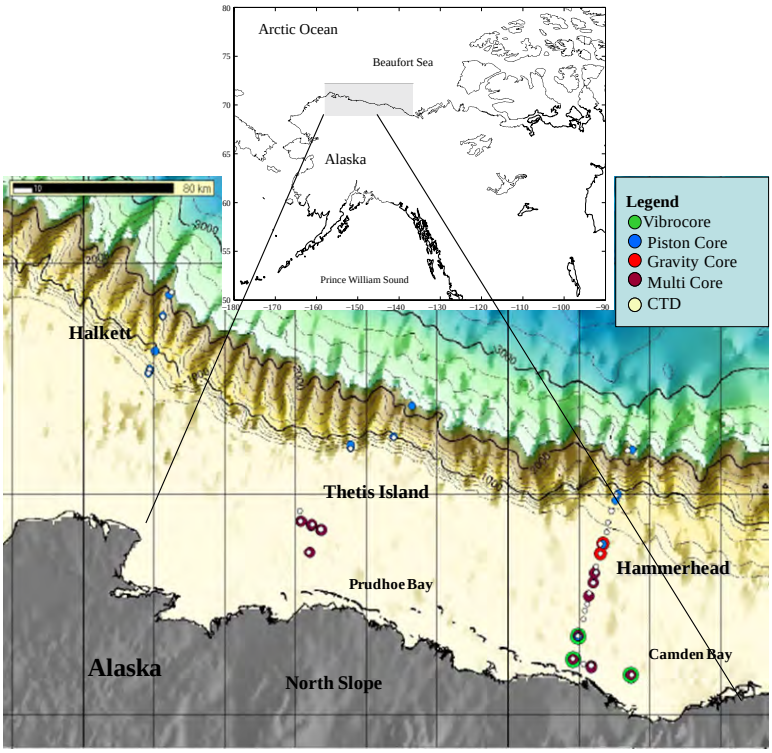

Figure 1: Water column and sediment sampling locations for the MITAS 1 expedition in the Beaufort Sea off the coast of Alaska.

across the Alaskan coast (Figure 1). The initial planning for nearshore to offshore transects for the sediment and water column sampling was staged with an MMS data review by B. Herman, R. Coffin, W. Wood, K. Rose, and P. Hart (Appendix 3). Considerations for the site selections included review of the presence of mounds, lithostratigraphy and sub-seafloor geologic structures, seismic data, wire-line logs when available, and previously published studies.

IV. Methods

A. Core Site Selections – Piston coring and vibrocoring was conducted at 4 distinct locations across the US region of the Beaufort Sea (Figure 2, Table 1). MMS and USGS high-resolution seismic profiles were surveyed to detect pockets of gas from dissociating hydrate and indications of deep sediment methane hydrate deposits. Gas in sediments is known to generate strong reflections or diffractions. Field sampling was focused to investigate shallow sediments gas pockets located in the permafrost and top of gas hydrate stability (TGHS). Gas around the TGHS suggests on-going gas hydrate dissociation, whereas gas that is present well above the TGHS but within the permafrost may be caused by meta-stable gas hydrates. Offshore we investigated seismic profiles for possible gas at the base of gas hydrate stability (BGHS), leading to bottom simulating reflections (BSRs). BSRs were used as a scale evaluation of deep sediment hydrates and are still the best indicators on regional scales for the presence of a gas hydrate system.

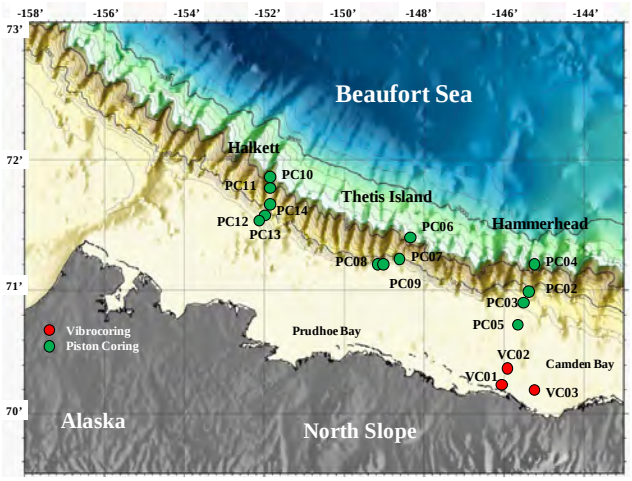

Figure 2: Coring was done at 4 locations across the Beaufort Sea.

B. Analyses of Vertical Methane Fluxes – Vertical methane flux profiles were surveyed through regions above the permafrost and over coastal hydrate beds. An overview of the research focus for this effort is presented in Appendix 4. Piston coring and vibrocoring were used to retrieve sediment samples. Sediment porewater profiles were analyzed on board for methane (CH_4), sulfate (SO_4^{2-}), dissolved inorganic carbon (DIC), total sulfide (TDS) and chloride (Cl^-) concentrations to estimate the vertical methane flux. These data provide an indirect estimate of sediment anaerobic oxidation of methane (AOM) which occurs where vertical flow of deep sediment CH_4 and shallow sediment SO_4^{-2} converge at the sulfate methane transition (SMT). Above the SMT, SO_4^{-2} concentrations increase toward seawater concentrations at the sediment-water column interface, while below, CH_4 concentrations increase due to *in situ* methanogenesis or diffusion and advection from deeper sources. While the SMT provides a qualitative prediction of vertical CH_4 diffusion and advection, quantitative estimates of vertical CH_4 flux can be calculated from analysis of the SO_4^{-2} gradient. Diffusive flux calculations from the linear SO_4^{-2} porewater profiles and sediment porosity are applied according to Fick's first law assuming steady state conditions. These calculations enable a spatial description of the vertical methane flux onboard to assist in the core site selection.

C. Sediment Processing - Whole core sections were cut from piston and vibrocore barrel sleeve sections. Sample selection through the core was based on the visual identification of sediment sections containing sulfide (dark sediment) and/or core gas pockets. Fewer samples were taken toward the sediment-water column interface and sample resolution increased toward the SMT; 15 to 20 samples were taken in each core. Porewater collection was conducted using Rhizon samplers drawn with 20 ml syringes. Core cutting and sample distribution procedures are presented in Appendix 5.

Porewater sub-sample collection for data presented in this report include 1 ml taken for total sulfide concentrations, then 2 ml was transferred into serum vials for DIC concentration, and 2-3 ml was transferred into separate vials for δ^{13}C-DIC. These vials are sealed immediately with Teflon septa. Finally, 2 ml is transferred into a screw-top vial for ion analysis (SO_4^{-2} and Cl^-). DIC concentration samples were analyzed onboard, and were frozen if not analyzed immediately following sampling. The ion samples were refrigerated until they were analyzed onboard and δ^{13}C-DIC samples were frozen for analyses back in the lab. A total sediment and porewater sample distribution is presented in Appendix 6; some of the sample splits varied during the cruise, depending on the volume obtained.

D. On Board Pore Water Analyses - The following porewater analysis was conducted on board:

i. Sulfate and Chloride Concentrations – Sulfate and chloride concentrations were measured with a Dionex DX-120 ion chromatograph equipped with an AS-9HC column. Samples were diluted 1:50 (vol/vol) prior to analysis and measured against a 1:50 diluted IAPSO standard seawater (28.9 mM SO_4^{-2}, 559 mM Cl^-). Sulfate and chloride are presented in millimolar units (mM). Limits of detection are <0.1 mM.

ii. Sediment Methane Concentrations - Methane concentrations were determined from 3-ml sediment plugs using headspace techniques and were quantified against certified gas standards (Scott Gas, Plumbsteadville PA). Headspace analysis was performed on board using a GC-FID Shimadzu GC-14A gas chromatograph equipped with a 6 foot by 1/8 inch HayeSep-Q 80/100 column. Methane concentrations are presented in millimolar units (mM).

iii. Sulfide concentrations - Pore water sulfide concentrations were measured with a Turner spectrophotometer, using the Cline method (Cline, 1969). Sulfide concentrations are presented in millimolar units (mM).

iv. Pore Water DIC Concentrations - Pore water dissolved inorganic carbon (DIC) concentrations were measured using a UIC coulometer and standardized against a certified reference material (CRM, Batch 58). DIC concentrations are presented in millimolar units (mM).

V. Results

This data summary focuses on the sediment core porewater profiles for CH_4, SO_4^{2-} and DIC concentrations, from 4 different regions; Hammerhead offshore, Hammerhead nearshore, Thetis Island, and Halkett (Figure 2, Table 1). All of the porewater data are presented in Appendix 7. Station coordinates and water column depth for each location are presented in Table 1. Selection of all of core locations was based on precruise review of MMS seismic data and onboard 3.5 kHz profiles taken from the system onboard the *USGSC Polar Sea.* The primary goal for this data set was to establish spatial variation in the vertical methane flux from deep sediments offshore and shallow permafrost hydrates in the nearshore sediment. The spatial variation in the vertical CH_4 flux will be used to interpret the shallow sediment carbon cycling, spatial variation in the microbial community diversity, and the transport to the overlying water column. Hammerhead nearshore sediment samples were taken with a vibrocore. All other cores were retrieved with a piston core.

Table 1: Core location, date and water column depth

CORE ID	Date	Latitude	Longitude	Water Depth (m)
VC02	19-Sep-09	70° 21.6448' N	146° 00.4635' W	20
VC03	19-Sep-09	70° 15.34210' N	146° 04.69180' W	22
PC02	20-Sep-09	71° 00.22810' N	145° 27.03660' W	566
PC03	20-Sep-09	70° 58.47840' N	145° 29.21420' W	490
PC04	21-Sep-09	71° 11.98460' N	145° 14.95110' W	2077
PC06	22-Sep-09	71° 23.53660' N	148° 21.52630' W	2208
PC07	22-Sep-09	71° 15.32580' N	148° 36.93170' W	985
PC08	23-Sep-09	71° 12.44330' N	149° 13.46600' W	144.5
PC09	23-Sep-09	71° 13.14430' N	149° 13.23340' W	306
PC10	24-Sep-09	71° 52.04010' N	151° 46.91160' W	1957
PC11	25-Sep-09	71° 46.68280' N	151° 52.70670' W	1458
PC12	25-Sep-09	71° 32.97120' N	152° 03.68110' W	342
PC13	25-Sep-09	71° 31.86300' N	152° 04.75420' W	280
PC14	25-Sep-09	71° 37.64200' N	151° 59.29430' W	1005

Hammerhead was initially selected because of previous industrial exploration drilling and the availability of a large seismic data set. Seismic data were used to select the Hammerhead drill site nearshore vibrocore locations. Figure 3 represents a view of the general area and shows near sediment surface seismic mixing profiles indicative of shallow sediment gas. These regions overlie seismic blanking profiles that indicate deeper sediment fluid and/or gas fluxes. Based on these profiles seismic lines east of Hammerhead and along seismic line WB104 (Figure 3) were a focus region for the coring. At this location initial sediment sampling was done with the piston core system. The first core in the region resulted in a ship winch

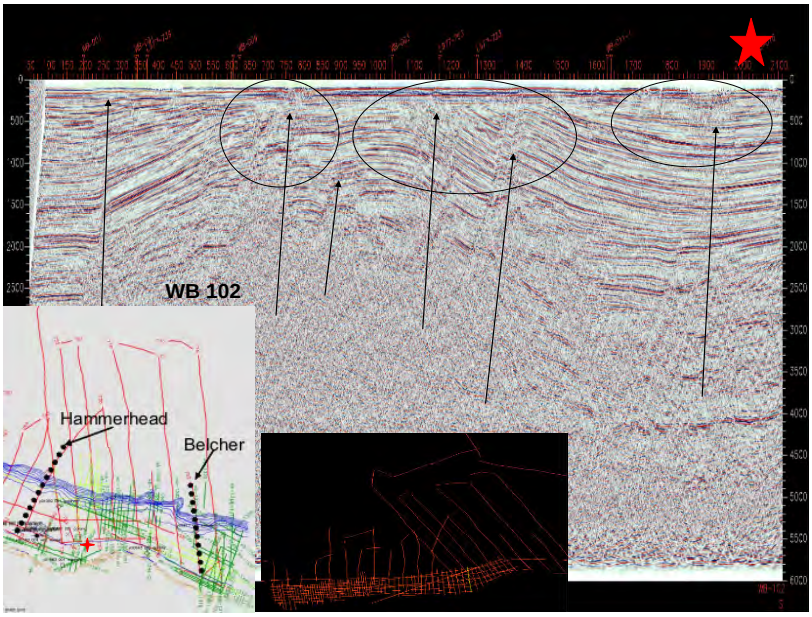

Figure 3: An example of nearshore seismic data the nearshore Hammerhead study region. The symbol ✧ represent the region where the seismic data were retrieved. Shallow sediment seismic blanking is circled and potential regions for vertical fluid and gas fluxes are shown with arrows.

failure and when the winch was restored, approximately 45,000 lbs of tension pull for recovery broke the cast wire. Subsequent coring in water column depths of 40 m or less was done with the vibrocore or multicore. Mutlicore data are not presented in this report.

The sediment CH_4 concentration from Hammerhead nearshore porewater ranged from 0.12 to 0.91 μM in VC02 and VC03 (Figure 4). While CH_4 concentrations in VC02 sediment porewater were higher there was no trend through individual profiles or between cores. Porewater SO_4^{2-} concentrations for Hammerhead nearshore ranged from 24.7 mM at surface down to 19.4 mM, in deeper VC03. The low change in concentrations through porewater CH_4 and SO_4^{2-} profiles were similar to the vertical variation in the porewater DIC which ranged from 4.16 mM to 12.3 mM. Highest DIC concentrations were observed through a down profile increasing concentration gradient in VC02. VC03 was fairly linear through the entire profile. Low variation in SO_4^{2-} profiles coupled with low CH_4 concentrations and no high increase in the DIC profile through the cores suggest minimum to no AOM at this location. VC01 was dry and sediment porewater could not be extracted.

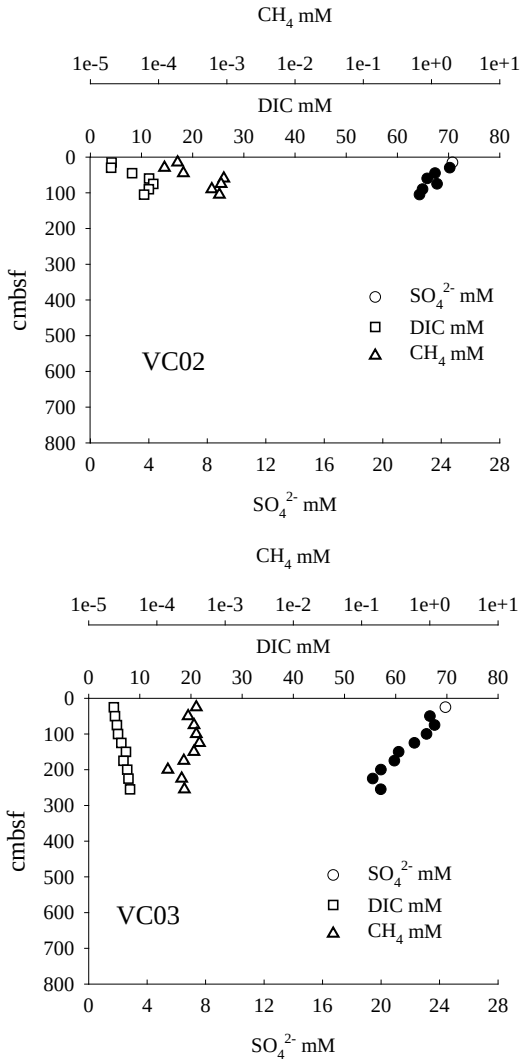

Figure 4: Hammerhead nearshore porewater profiles.

Moving offshore from Hammerhead permafrost vibrocoring, piston cores were taken at water column depths of 490 m to 2077 m. Figure 5 presents seismic data review conducted for focus regions and the 3.5 kHz data obtained at sea to select the core locations. In the offshore region of PC04 3.5 kHz data were not collected and the focus area was based on the USGS seismic line. This region was observed to have a strong BSR and some regions with seismic blanking that suggested vertical gas and/or fluid fluxes. Core PC02 was taken at the edge of a sediment slope with a moderate shallow sediment blanking and PC03 was taken a short distance down slope.

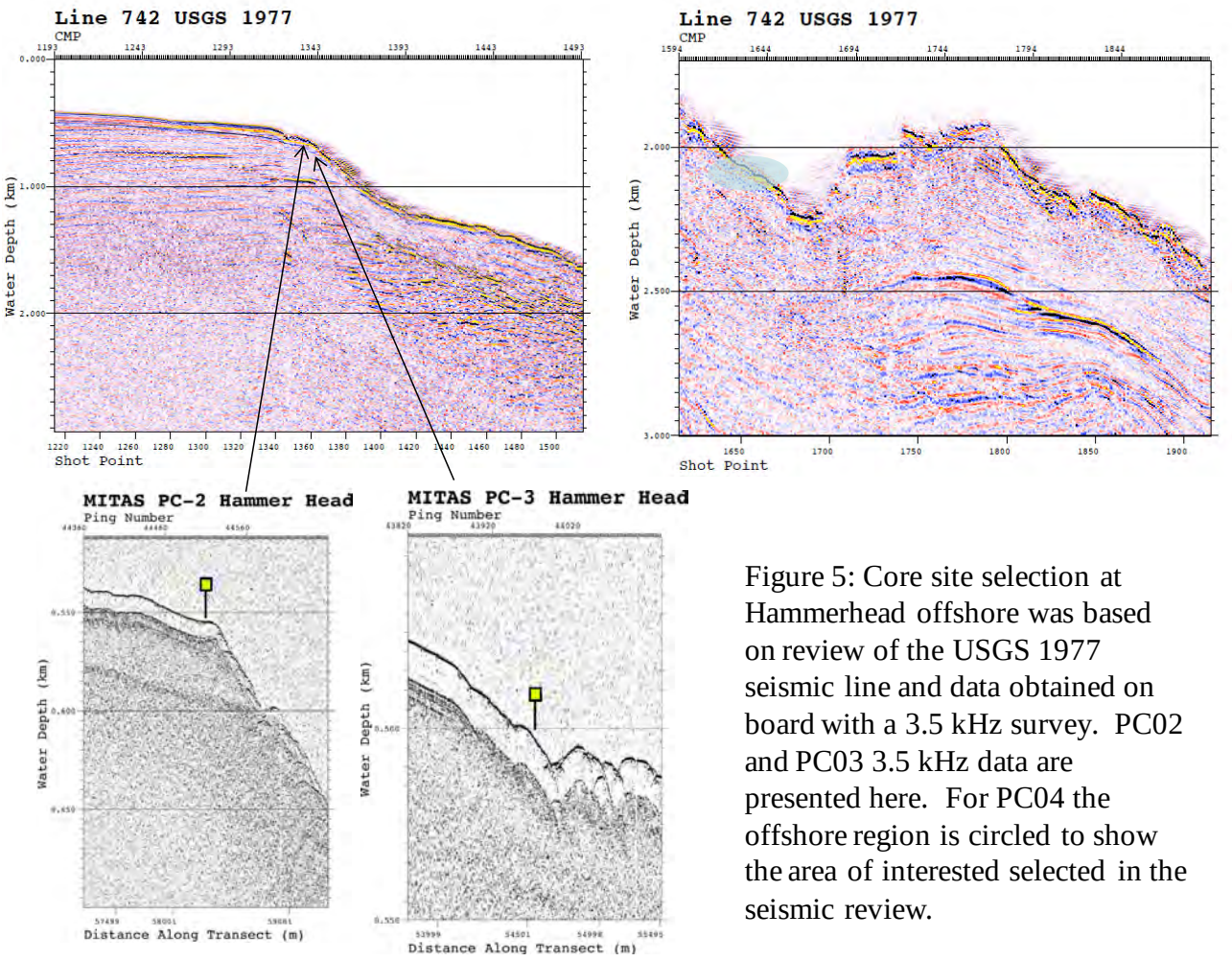

Figure 5: Core site selection at Hammerhead offshore was based on review of the USGS 1977 seismic line and data obtained on board with a 3.5 kHz survey. PC02 and PC03 3.5 kHz data are presented here. For PC04 the offshore region is circled to show the area of interested selected in the seismic review.

Offshore at Hammerhead low CH_4 fluxes, similar to nearshore Hammerhead, were also suggested by porewater CH_4, SO_4^{2-}, and DIC profiles (Figure 6). Concentrations of CH_4 through all of the cores ranged from 0.08 μM to 10.7 μM with the highest values measured in the offshore core from a water column depth of 2077 m. SO_4^{2-} profiles through all of the cores were similar to the nearshore permafrost region, with a range of 26.5 mM at the surface down to a minimum concentration of 19.6 mM in PC03 at 675 cmbsf. Through PC02 with a core depth of 661 cm, the total concentration range from surface to bottom was 27.9 mM to 26.0 mM. Porewater DIC also did not show large concentration gradients through these vertical profiles (Figure 6); with a minimum core surface concentration of 3.7 mM and a maximum down core concentration of 10.2 mM in PC03. While a slight mid core increase in the DIC concentration was observed in PC02 and PC03 these were low ranges in the concentrations. Moving further offshore PC03 was observed to have a similar profile in CH_4, DIC and SO_4^{2-} (Figure 6).

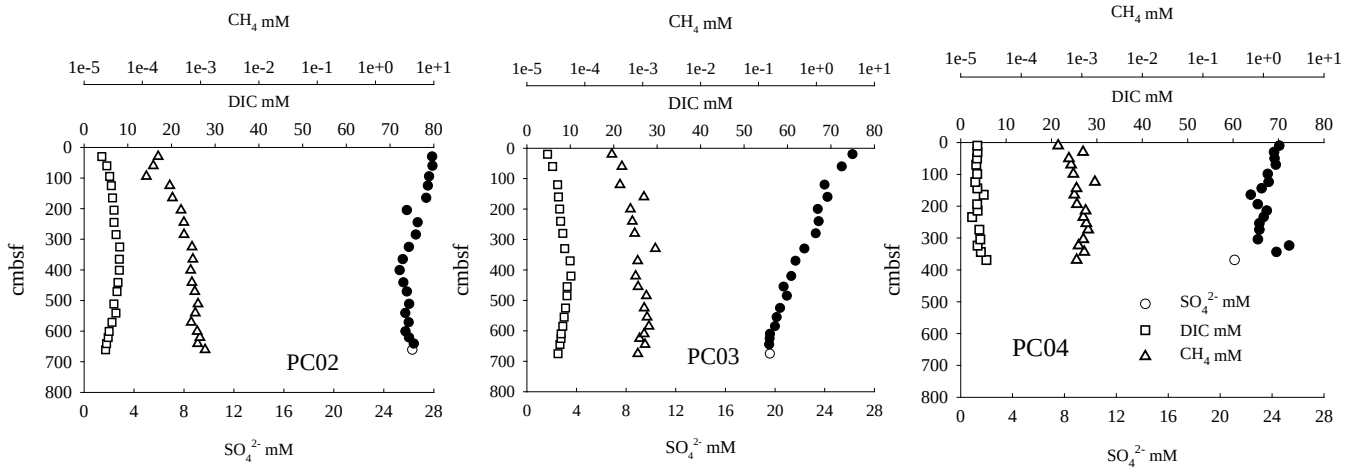

Figure 6: Hammerhead offshore porewater profiles.

Moving west to Thetis Island, piston cores PC06, PC07, PC08 and PC09 were taken at across the shelf at water column depths ranging from 306 m to 2208 m (Table 1, Figure 7). Core locations were selected on the basis of spatial variation in the shallow seismic blanking that suggests shallow permafrost sediment gas, vertical blanking that indicated vertical gas and fluid flux, and deeper sediment BSR indicating regions where hydrates were stable in the sediment.

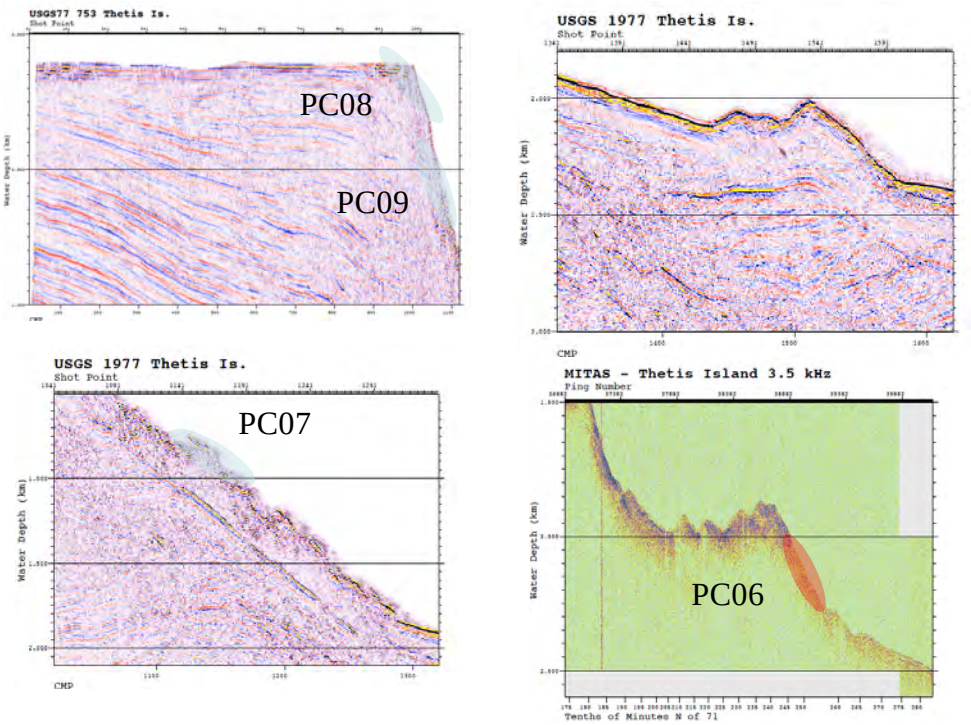

Figure 7: Thetis Island piston core site selection basic on 1977 USGS seismic data for PC07, PC08 and PC09. PC06 selection was based on the onboard 3.5 kHz data taken over the previous USGS seismic profiles. Approximate regions for the coring is highlighted.

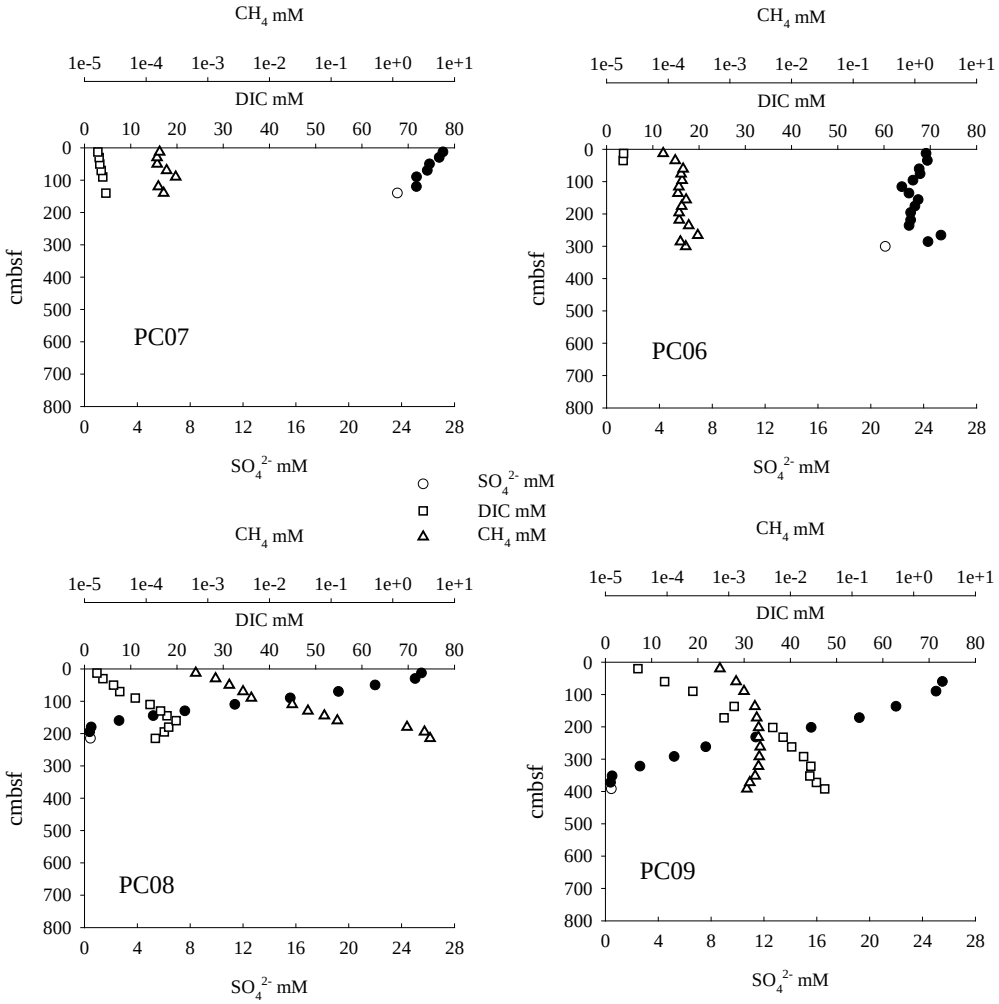

Figure 8: Thetis Island porewater profiles

At core locations around Thetis Island the CH_4 concentrations ranged from 0.1 μM to 4.0 mM (Figure 8). The highest CH_4 in this region was observed through the PC08 profile with a range from 0.64 μM in the shallow section and up to 4.0 mM at 160 cmbsf. Porewater SO_4^{2-} from cores around Thetis Island ranged from 27.1 mM at the surface down to 0.08 μM deeper in the core. Core depths with minimum SO_4^{2-} concentrations were observed at 180 cmbsf and 392 cmbsf for PC08 and PC09, respectively. Similar to offshore and nearshore locations for Hammerhead PC06 and PC07 SO_4^{2-} profiles showed little change in concentration through the core. Shallow core porewater DIC around Thetis Island ranged from 2.7 mM to 7.1 mM. Through the vertical DIC profile there was little change in concentration for PC07. PC06 samples were lost and will be rerun. DIC in PC08 showed a rapid increase in concentration, up to 19.8 mM at 160 cmbsf that varied with SO_4^{2-} and CH_4 profiles (Figure 8). The increase in PC09 DIC was observed deeper with a concentration of 47.4 mM at 392 cmbsf. The decline in SO_4^{2-} simultaneous with increase in DIC suggests the bottom of the core was near the SMT.

The final region for geochemical focus in this expedition, Halkett, was located west of the other sample regions (Figure 2). Piston cores were taken across the slope at water column depths ranging from

280 m to 1957 m (Table 1, Figure 9). Selection of the core sites was based on observation of strong BSRs and vertical blanking in the seismic profiles that suggested vertical fluid and gas migration.

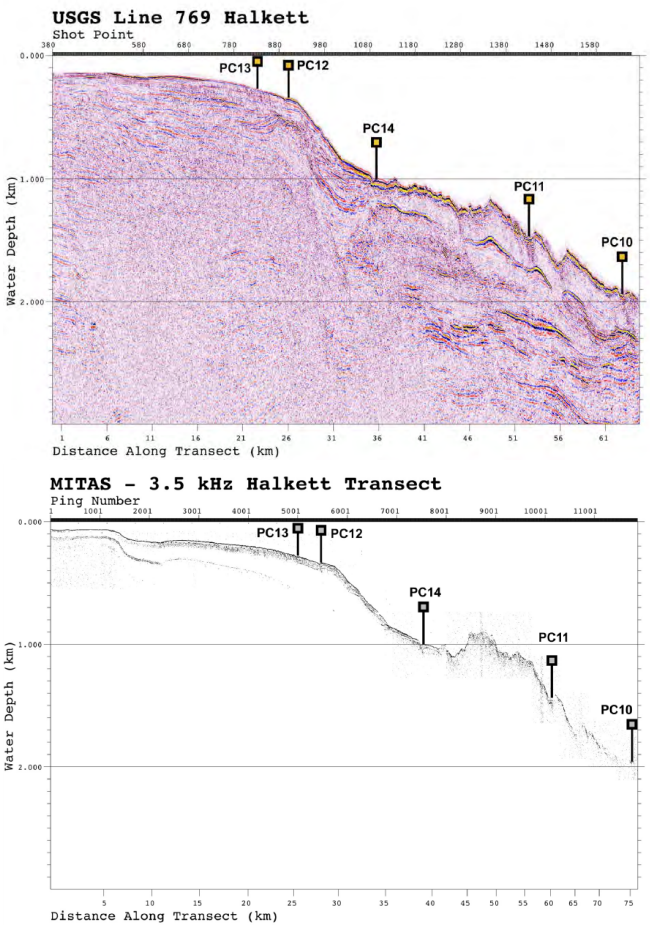

Figure 9: USGS 1977 and onboard 3.5 kHz for used for core site selection through the Halkett transect.

Halkett sediment geochemical profiles are presented in the Figure 10. Porewater CH_4 concentrations for these cores were generally higher with a range in concentration of 0.12 μM to 12.6 mM. PC10 and PC11 located in the deepest water for this region had the lowest CH_4 concentrations. In contrast there was a large increase in CH_4 concentrations in core bottom samples from PC12, PC13 and PC14. Linear SO_4^{2-} profiles were observed in all of the cores with a wide range in slopes starting at a shallow sediment concentration of 25 to 27 mM. Further offshore minimum concentrations were measured at 9.1 mM at 546 cmbsf in PC11. Nearshore minimum concentrations of 0.3 μM to 0.5 μM were measured at 405 cmbsf, 110 cmbsf and 220 cmbsf for PC12, PC13 and PC14, respectively.

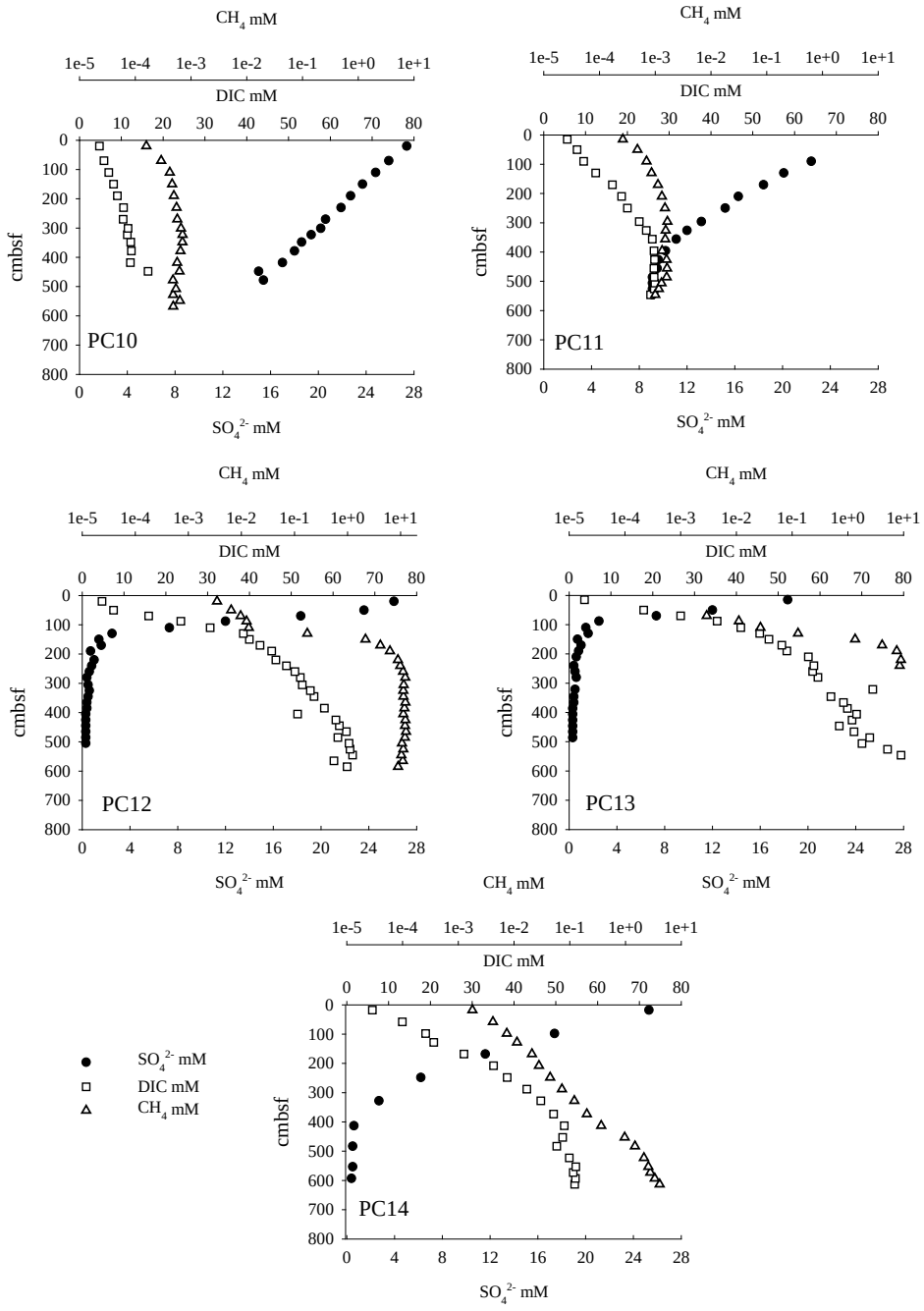

Figure 10: Halkett porewater profiles

A summary of the CH_4, SO_4^{-2} and DIC profiles provide a spatial overview of variation in vertical CH_4 fluxes (Table 2). The lowest CH_4 flux estimated with the downward SO_4^{-2} diffusion was observed in the offshore Hammerhead core sites with a range from -2.03 to- 6.09 mM SO_4^{2-} m^{-2} a^{-1}. There was an increase in the SO_4^{-2} diffusion moving nearshore over the permafrost Hammerhead area with values at approximately -15 mM SO_4^{2-} m^{-2} a^{-1} (Table 2). The SO_4^{2-} diffusion increased at the westward location of Thetis Island with a range of -2.0 to -100 mM SO_4^{2-} m^{-2} $a^{-1}$and the lowest value being observed in PC06 located offshore in the Beaufort Sea with an overlying water column depth of 2207 m. Finally, at Halkett,

the furthest west core transect the range of SO_4^{2-} diffusion ranged -17.7 to -155 mM SO_4^{2-} m^{-2} a^{-1}. The highest downward SO_4^{2-} diffusion was observed nearshore at PC12 and PC13.

Table 2: Estimates of the sulfate-methane-transition (SMT) and downward sulfate diffusion for core locations in the Beaufort Sea.

Core	SMT (cmbsf)	SO_4^{2-} mM m^{-2} a^{-1}
VC02	854	15.4
VC03	979	15.2
PC02	5051	2.34
PC03	2390	6.09
PC04	2905	2.06
PC06	3841	2.03
PC07	1053	15.9
PC08	179	100.1
PC09	351	37.7
PC10	1036	17.7
PC11	629	27.4
PC12	147	124.7
PC13	106	154.8
PC14	373	44.2

VI. Summary

This report provides background sediment and porewater data for the interpretation of the MITAS I expedition. There is a strong spatial variation in the vertical methane flux, with highest values measured in the Halkett region sediment. Lowest coastal vertical CH4 fluxes were observed at Hammerhead and all nearshore data was flux data at a similar, low level. Data will be available for assistance in interpretation of the following research topics addressed during our expedition.

- Comparison of vertical methane fluxes in nearshores permafrost sediment relative to offshore deep sediment hydrate deposits.
- Overview of Beaufort Sea shelf methane hydrate distribution for future energy studies.
- Spatial variation in methane contribution to shallow sediment carbon cycling.
- Sediment methane flux to the water column and atmosphere.
- Methane influence on microbial community structure diversity.

Future studies will address the low sediment methane fluxes observed in the nearshore tundra and a more thorough evaluation of deep sediment methane hydrate deposits around Halkett.

VII. Literature Cited

Carmack, E. C. and R. W. MacDonald. 2002. Oceanography of the Canadian Shelf of the Beaufort Sea: A Setting for Marine Life. Arctic. 56:29-45.

Cline, J. D. 1969. Spectrophotometric Determination of Hydrogen Sulfide in Natural Waters. Pp. 454-458, Limnology and Oceanography.

Dickens, G. R., J. R. O'Neil, K. K. Rea. and R. M. Owen. 1995. Dissociation of oceanic methane hydrate as a cause of the carbon isoptope excursion at the end of Paleocene. Paleoceanogpraphy, 10:965-971.

Dunton, K.H., Weingartner, T., and Carmack, E.C., 2006. The nearshore western Beaufort Sea ecosystem: circulation and importance of terrestrial carbon in arctic coastal food webs. Progress in Oceanography 71:362–378.

Frey, K. and L. C. Smith. 2005. Amplified carbon release from vast West Siberian peatlands by 2100. Geophy. Res. Let. 32, L09401.

Gorham, E. 1991. Northern peatlands: Role in the carbon cycle and probable responses to climatic warming. Ecol. Appl. 1:182-195.

Kennett, J. P., K. G. Cannariato, I. L. Hendy, and R. J. Behl. 2002. Methane Hydrates in Quaternary Climate Change The Clathrate Gun Hypothesis. American Geophysical Union, Washington, DC, 224 pp.

Kvenvolden, K. A. 1999. Potential effects of gas hydrate on human welfare. Proc.Natl.Acad.Sci.U.S.A. 96: 3420-3426.

Kvenvolden, K. A. 2003. Natural gas hydrates: introduction and history of discovery In M.D.Max (Ed). Natural gas hydrate in oceanic and permafrost environments. Kluwer Academic Publishers, 9-16.

Max, M.D. & Lowrie, A. 1993. Natural gas hydrates: Arctic and Nordic Sea potential. In: Vorren, T.O., Bergsager, E., Dahl-Stamnes, Ø. A., Holter, E., Johansen, B., Lie, E. & Lund, T.B. Arctic Geology and Petroleum Potential, Proceedings of the Norwegian Petroleum Society Conference, 15-17 August 1990, Tromsø, Norway. Norwegian Petroleum Society (NPF), Special Publication 2 Elsevier, Amsterdam, 27-53.

Milkov,A.V. and R.Sassen 2003. Preliminary assessment of resources and economic potential of individual gas hydrate accumulations in the Gulf of Mexico continental slope. Marine and Petroleum Geology 20: 111-128.

Rothwell, R. G., J. Thompson, and G. Kahler. 1998. Low-sea-level emplacement of a very large late Pleistocene 'megatirbodote' in the western Mediterranean Sea. Nature 392:377-380.

Shakhova, N., I. Semiletov, and G. Panteleev. 2005. The distribution of methane on the Siberian Arctic shelves: Implications for the marine methane cycle. Geophysical Research Letters, 32: L09601, doi:10.1029/2005GL022751, 2005.

Sower, T. 2006. Late Quaternary Atmospheric CH_4 Isotope Record Suggests Marine Clathrates Are Stable. Science 311:838-840.

APPENDIX 1: Description of the *USCG Polar Sea* contracted for this expedition.

POLAR SEA (Table 1) is equipped to function as a major scientific platform with five internal laboratories and accommodations for as many as thirty-five scientists and technicians. POLAR SEA can accommodate an additional seven portable science laboratories on deck. Real-time satellite images processed aboard aid in ice navigation, science planning and weather forecasting. The vessel is set with dynamic positioning for field work. While not in the initial planning, helicopter operations are possible for transporting scientists to and from the field.

Table 1: *USCG Polar Sea* Specs.

Basic Hull Characteristics	
Length Overall	399'
Maximum Draft	33'
Extreme Breadth	83' 6"
Full Load Displacement	13,227 Long Tons
Top of Mast above Waterline	138' 2"
Height of Eye from Bridge above Waterline	55' (8.7nm to horizon)
Height of Eye from Aloft Conn above Waterline	104' (12nm to horizon)
Max Sustained Open Water Speed	17.5 Knots
Power Train Information	
# of Diesel Electric Engines	6
# of Gas Turbines	3
# of Shafts	3
Horsepower per Shaft	
1 Diesel Engine/Shaft	3,000 hp Continuous
2 Diesel Engine/Shaft	6,000 hp Continuous
1 Gas Turbine/Shaft	20,000 hp Continuous
	25,000 hp demand boost

APPENDIX 2: Science team and research focus

The current plan for onboard instruments and support equipment is outlined in Table 2. Additional science equipment will be added to the expedition planning.

Table 1: This information will continue development through the cruise planning.

Item	**General Information**	**Users**
Seismic systems	Multibeam, MCS, SCS	Pecher, Wood, Greinert
Piston core/Vibrocore systems	9-12 m barrel system	Lorenson, Downer, Coffin
Multi-sensor core logger	Physical properties	tbd
XRD/XRF; Petrographic microscopes	Sedimentology/Lithostratigraphy	Rose, Johnson, Smith
Core processing van	All core processing and press included	Hamdan, Treude, Masutani, Coffin
Porewater chemistry lab	DIC, H_2S, Cl^-, SO_4^{-2}, CH_4	Hamdan, Lorenson
Seismic data processing lab	Computers and graphics	Pecher, Wood, Greinert
Heatflow probe	3 m probe	Wood, Downer
Radio-isotope tracer van	S-35, H-3, C14	Kirchman, Treude
CTD casts & water sampling	30L bottles, T, S, depth, fluorescence, particles, methane, nutrients, oxygen	Osburn, Kirchman, Greinert, Bianchi, Hamdan
Continuous surface seawater and air CH_4 measurements	TBD	TBD
Bubble fluxes	Hydroacoustic studies with single beam echosounder, bubble dissolution modeling	Greinert
Data compilation and methane flux model	Data integration in GIS and ODV, visualization in Fledermaus; modeling the fate of methane	Greinert, Coffin,Yvonne-Lewis, Osburn, Kirchman, Bianchi, Hamdan
Onboard acoustic experiments	Cores will be monitored for low frequency acoustic signatures with variation in gas flux	Wilson, Greene

Table 2: Scientific Party

	Scientist	Institution	Responsibility	Gender
1	Jonathan Borden	USGS-Woods Hole	ROV operations	M
2	Layton Bryant	Milibar HydroTest	Coring	M
3	Richard Coffin	NRL	CS/geochemistry	M
4	Matt Cottrell	University of Delaware	Water column methane	M
5	Sara Doty	USGS-Menlo	Sediments	F
6	Mara Dougherty	University of Maryland	Sediment radiocarbon	F
7	Ross Downer	Milibar HydroTest	Coring	M
8	Jens Greinert	NIOZ	Co-CS/ water column methane	M
9	Chad Greene	UT	Gas Flux Acoustics	M
10	Leila Hamdan	NRL	Microbial ecology	F
11	Pat Hart	USGS	seismics	M
12	Edna Huetten	NIOZ	water column methane	F
13	Joel Johnson	UNH	Sediment geology	
14	Dave Kirchman	University of Delaware	Water column	M
15	Chris Kinoshita	University of Hawaii	Sediment Processing	M
16	Stefan Krause	IFM-GEOMAR	Sediment microbial rates	M
17	Randy Larsen	St. Mary's College	Organic geochemistry	M
18	Curt Millholland	NRL	Core processing & lab analysis	M
19	Thomas Lorenson	USGS	Sediment Geochemistry	M
20	Rebecca Plummer	NRL/SAIC	Chemical lab	F
21	Jennifer Presley	NETL	Data archival and reporting	F
22	Koen de Rycker	RCMG	ROV ops	M
23	Kelly Rose	NETL	Co-CS/Lithostratigraphy	F
24	Sunita R Shah	NRL	Core processing & lab	F

			analysis	
25	Joe Smith	NRL	Inorganic geochemistry	M
26	Tina Treude	IFM-GEOMAR	Sediment microbial rates	F
27	Warren Wood	NRL	Co-CS/Seismics	M
28	Brandon Yoza	HNEI	Microbial ecology	M
29	Preston Wilson	UT	Acoustics, methane flux	M
30	Alaska Observer	TBD	TBD	TBD
31	COMPUTER TECH	TBD	TBD	TBD
32	CTD TECH	TBD	TBD	TBD

APPENDIX 3: Initial seismic data for sample station selection.

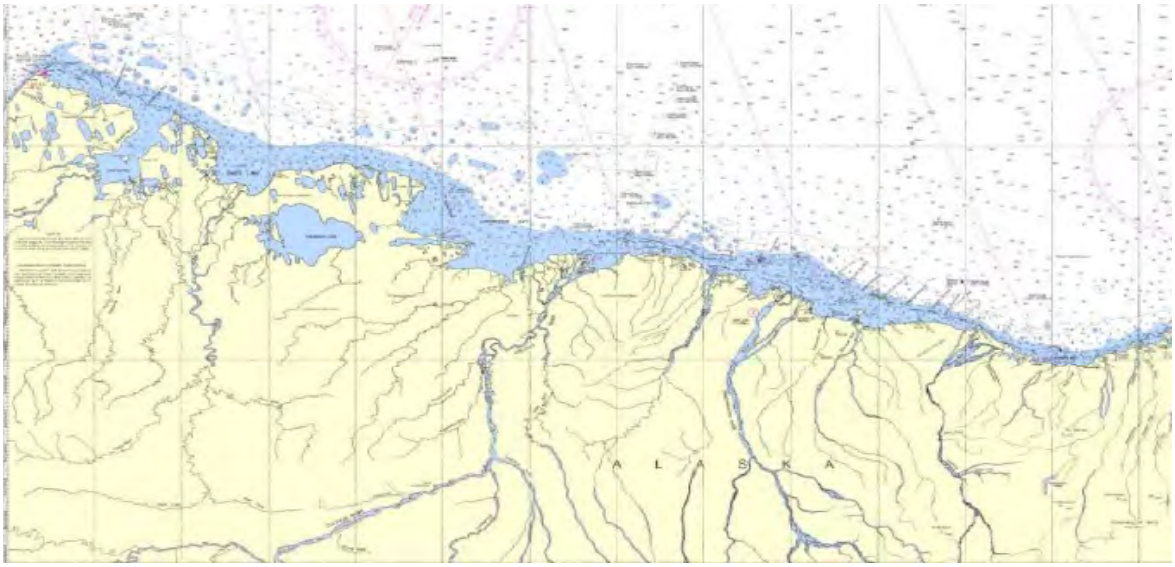

Figure 1: Off the northern coast of Alaska in the Beaufort Sea. The general field work region is off the coast of Barrow Alaska and runs eastward toward the MacKenzie Delta, between 71°49'N, 157°40'W' 71°20'N, 157°31'W; 71°23'N, 133°03'W; and 70°02'N, 113°39'W. Alaskan shelf morphology from the coast down to 1000 m and off the shelf down to 3500 m.

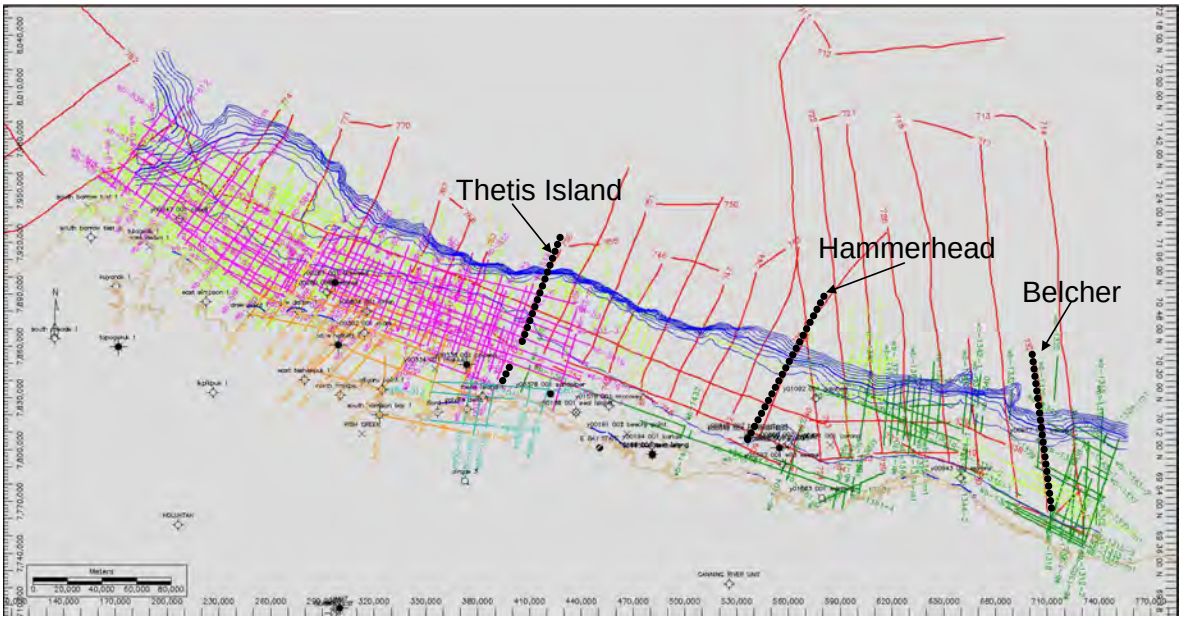

Figure 2: Locations for nearshore to offshore transects include Thetis Island Hammerhead and Belcher. Seismic lines were reviewed for exact locations. The following seismic charts are preliminary information for these sites. During the expedition additional sites were selected on the basic of the 3.5 kHz acoustic and shallow sediment geochemistry data.

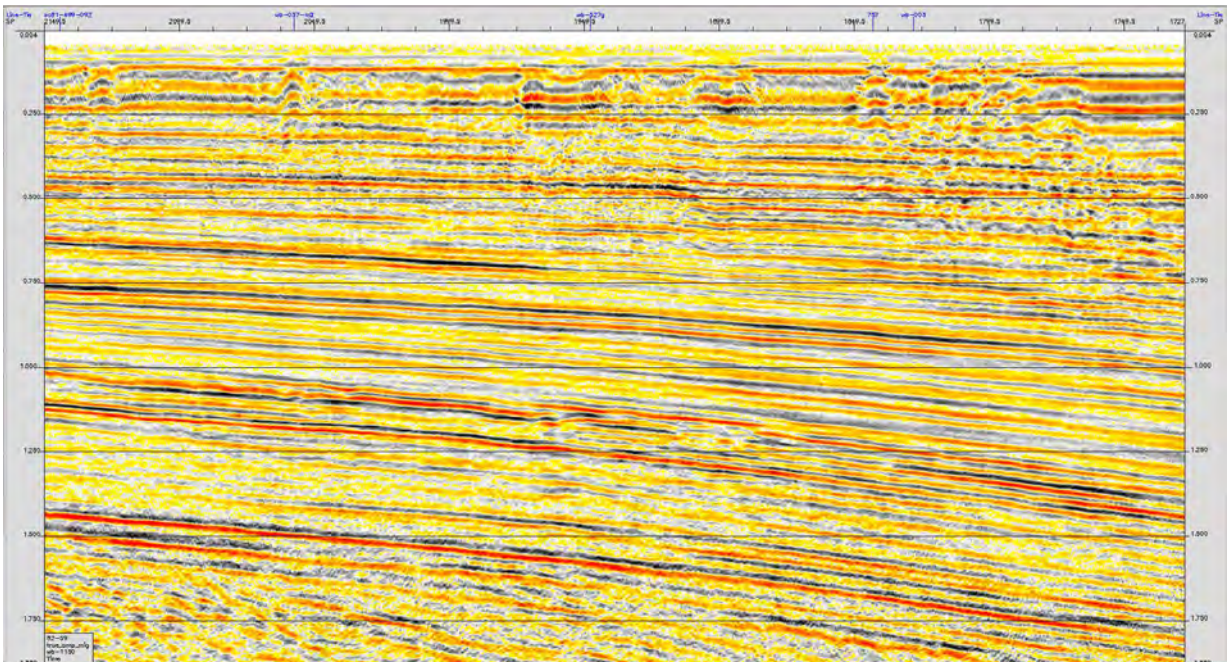

Figure 3: Example of seismic profile for Thetis Island.

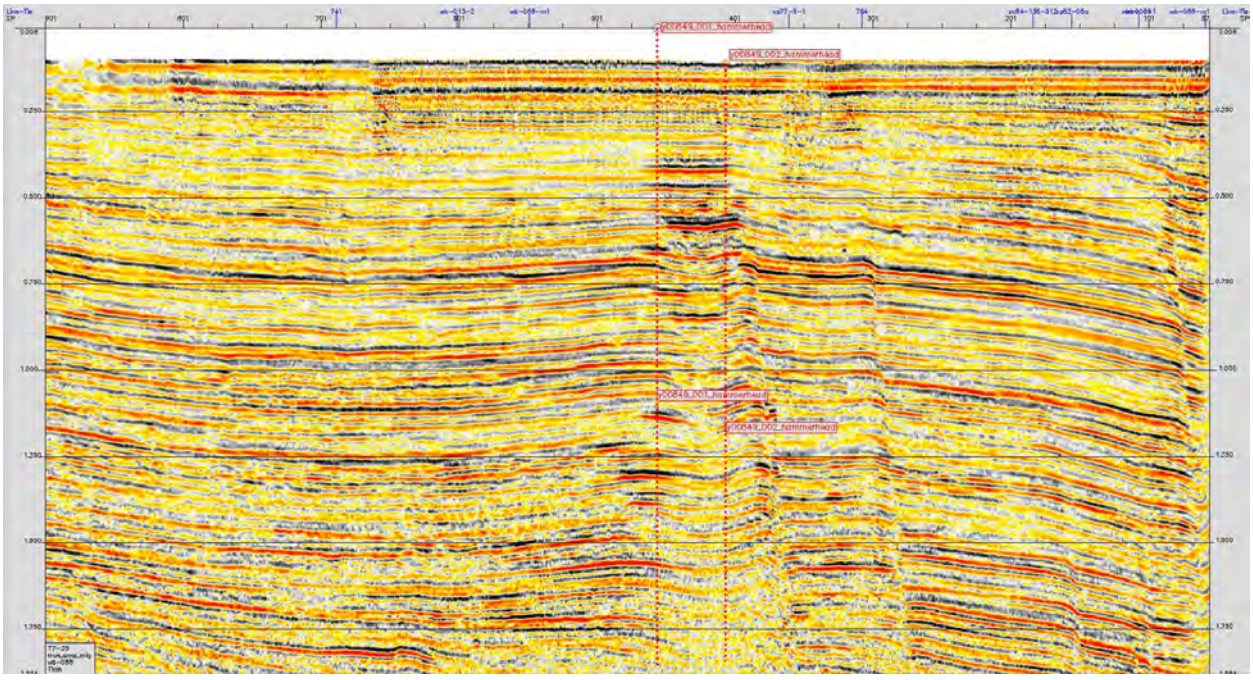

Figure 4.: Example of seismic profile for Hammerhead.

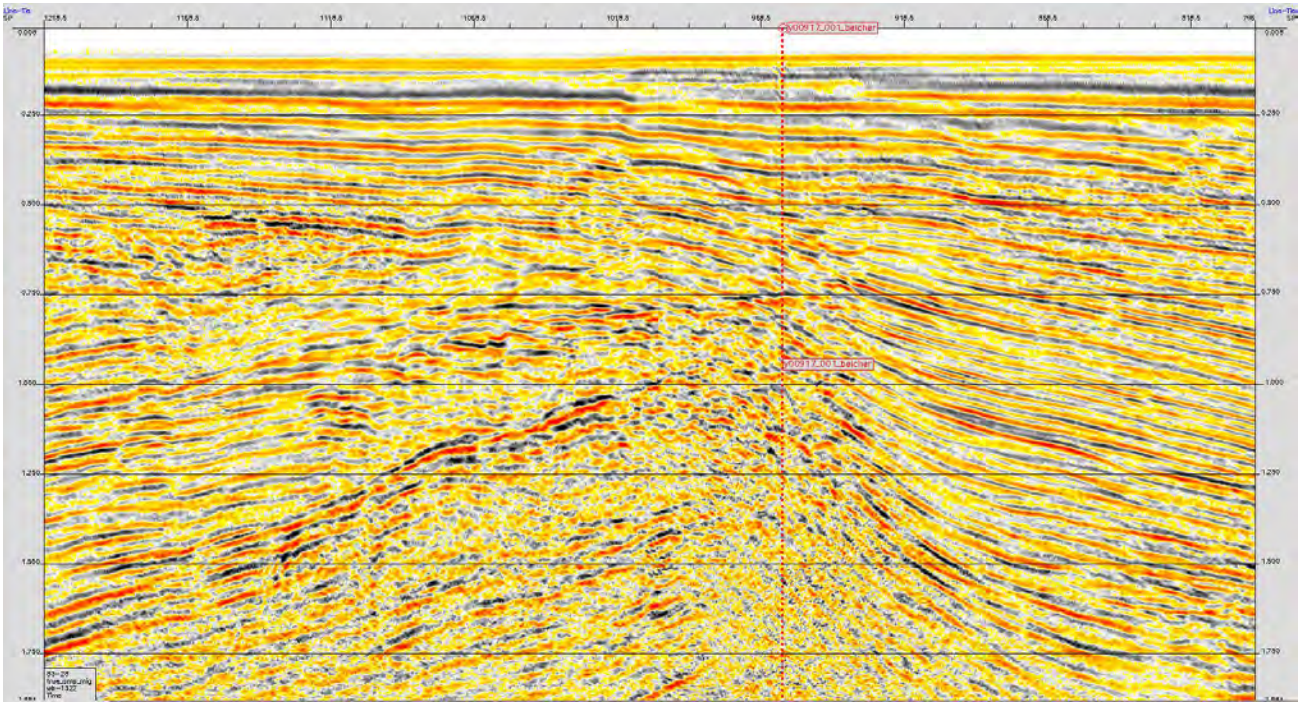

Figure 5. Example of seismic profile for Belcher.

APPENDIX 4: Research Overview

This expedition integrated a large array of biological, chemical and physical parameters to address the spatial variation of gas hydrate occurrence in the submerged permafrost. In addition, the project aims to constrain the methane contribution to the water column in shelf regions, carbon cycling in the sediment and the water column and finally the methane flux to the atmosphere (Figure 1). Specific research issues addressed by this program include:

A) Spatial variation of gas hydrate in nearshore to offshore seismic profiles for gas hydrate stability;

B) Lithostratigraphic and structural controls on sub-seafloor hydrate accumulations and ocean methane fluxes, coupled with geochemical summary of vertical methane fluxes, and the resulting shallow sediment methane cycling. This is compared in nearshore to offshore sediments for evaluation of vertical methane fluxes from deep sediments;

D) Spatial variation in bacterioplankton carbon cycling, related variation in microbial community diversity and the contribution of methane to microbial biomass;

E) Relative contribution of allochthonous tundra organic carbon and autochthonous primary production, to the nearshore organic carbon sources and spatial variation in the biotic and abiotic (e.g., photo-oxidation) variation in carbon cycling; and

F) Quantifying the amount of methane transported from the seafloor into the atmosphere via free or dissolved gas fluxes;

F) Setting up a numerical model that tracks the fate of methane in the sediment, through the water column and up into the atmosphere.

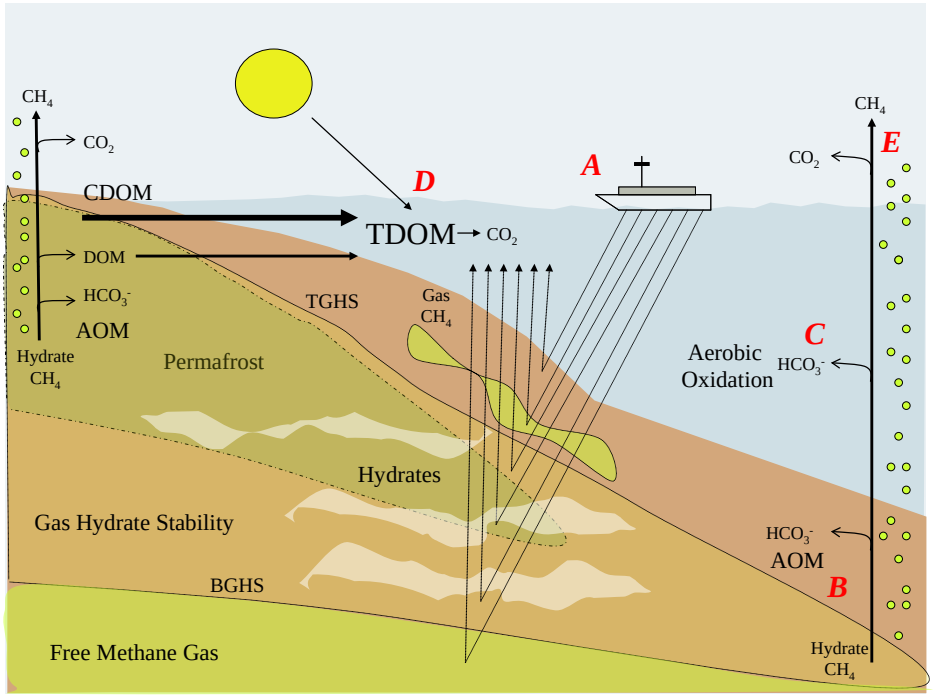

Figure 1: An integrated geophysics, geochemistry, and microbiology research plan designed to address the relative contributions of permafrost and coastal hydrate contributions to the sediment and water column carbon cycling and the spatial variation in the methane flux to the atmosphere. Abbreviations include DOM as dissolved organic matter, CDOM as colored dissolved organic matter, TDOM as total dissolved organic matter, AOM as anaerobic oxidation of methane, TGHS as the top of the gas hydrate stability and BGHS as the bottom of the gas hydrate stability.

APPENDIX 5: Core cutting guide

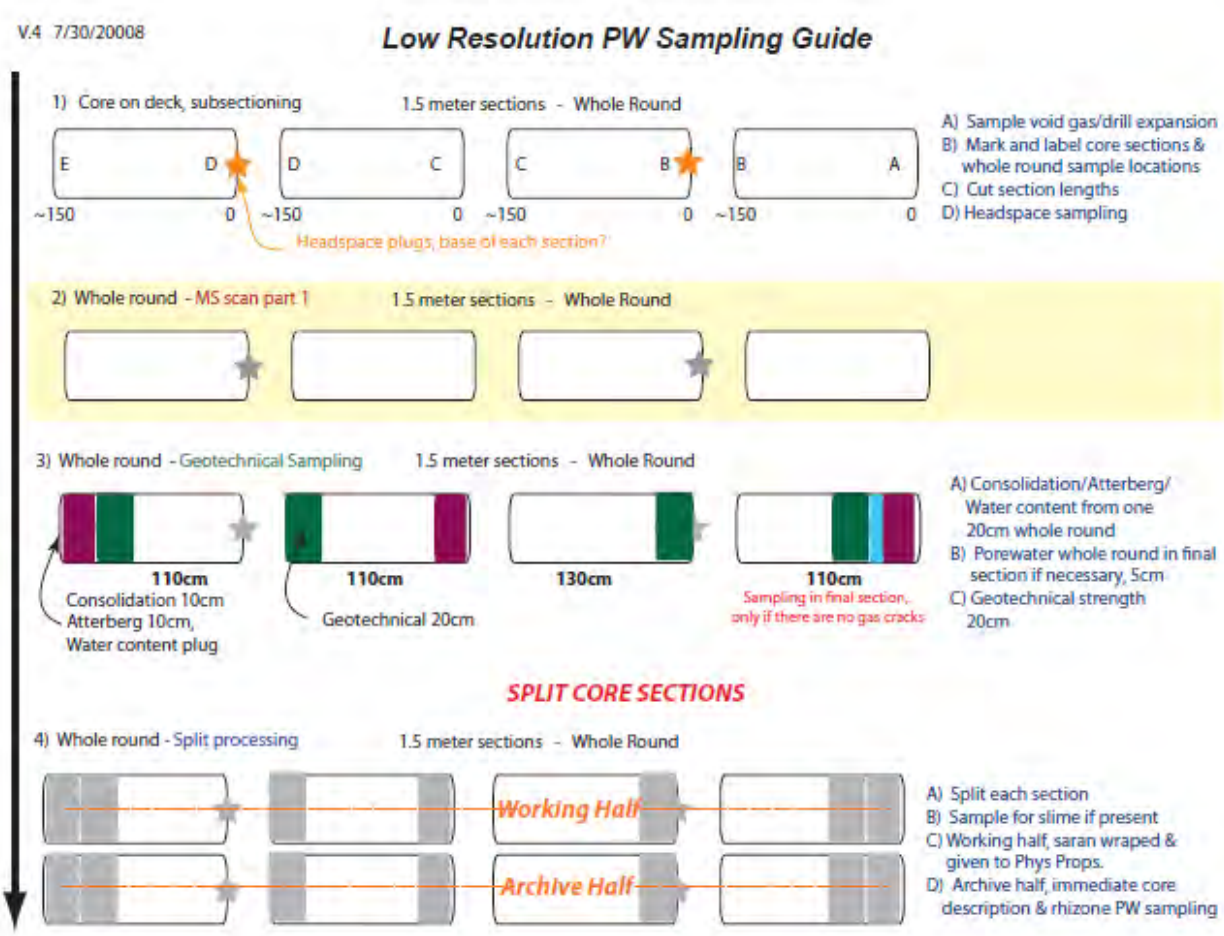

APPENDIX 6: Core Sediment and Porewater Processing

1. **Core sediment and Porewater processing –** The following information is on the sediment core processing for sediment and porewater samples.

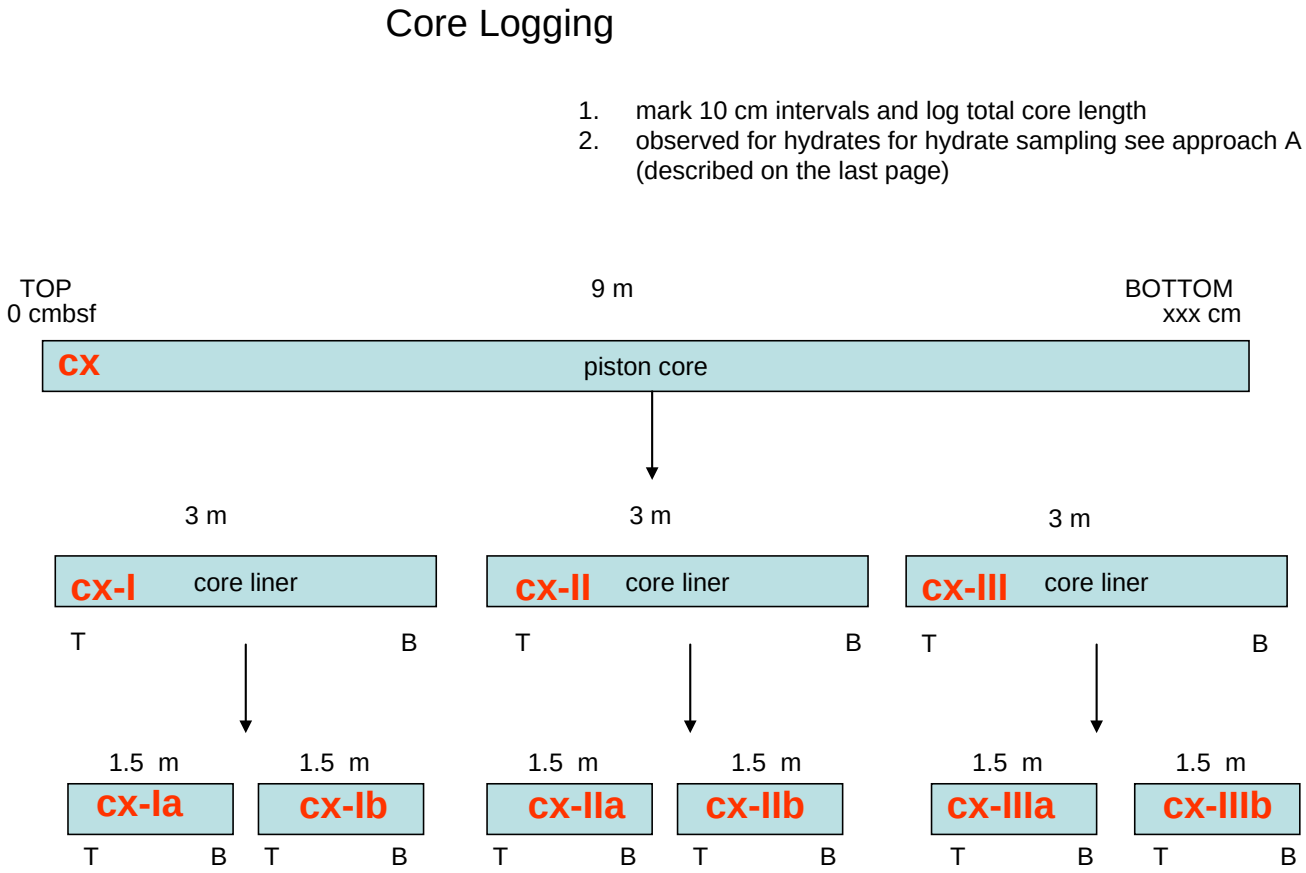

Subsamples for each parameter are labeled numerically with the lowest number at the top of each core. Each sub-core sample is labeled T for top and B for bottom. Observation of hydrates in the core will change the standard cutting operations. The letter x represents the core number (1, 2, 3, etc.)

Sub-core processing

150 cm sub section

0 10 20 30 40 50 60 70 80 150

CM

Each core sub-section will be processed through the following steps.

1. sediment gas pocket sampling on deck while sectioning, see approach B
2. core logger scan
3. Core sections horizontally split
4. methane sediment plug
5. rhizon porewater sampling
6. Working half, subsampled
7. Archive half:
   a) core imaging
   b) lithostrat description
8. Both halves frozen for shorebased work

A. Regions of cores that have hydrates will be excised from the core and hydrate will be frozen in liquid nitrogen. This region of the core will be noted in the core description.
B. Shallow drill through core sleeve with a 1/16 inch drill bit and collect gas with a 5 to 60 cc syringe.
C. Core sections will be split into working and archive halves
D. 3 ml coring syringe will be used for sampling from the working half, samples will be place in nitrogen sparged serum bottles and capped.
E. Rhizon porewater collection will be done after the core is split, this method will be tested before the cruise. Porewater presses will be brought for backup.
F. Working half will be used for additional sediment sampling
G. Archive half will be imaged and used for lithostratigraphic descriptions

general porewater sample distribution

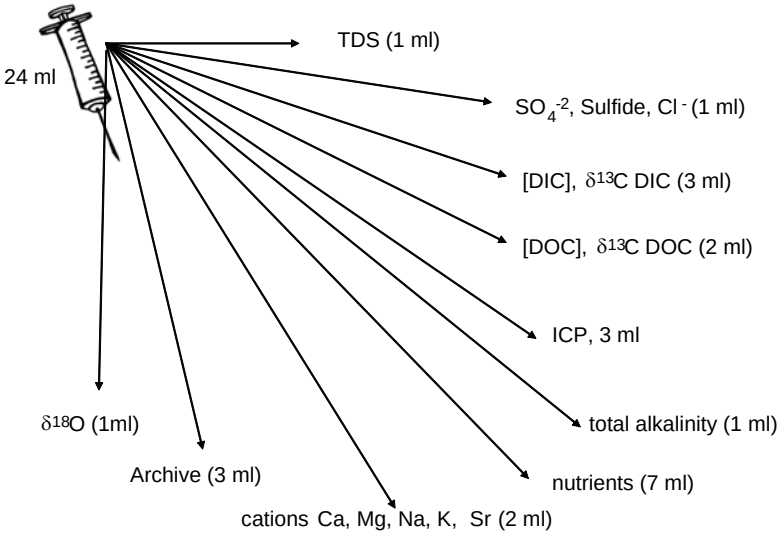

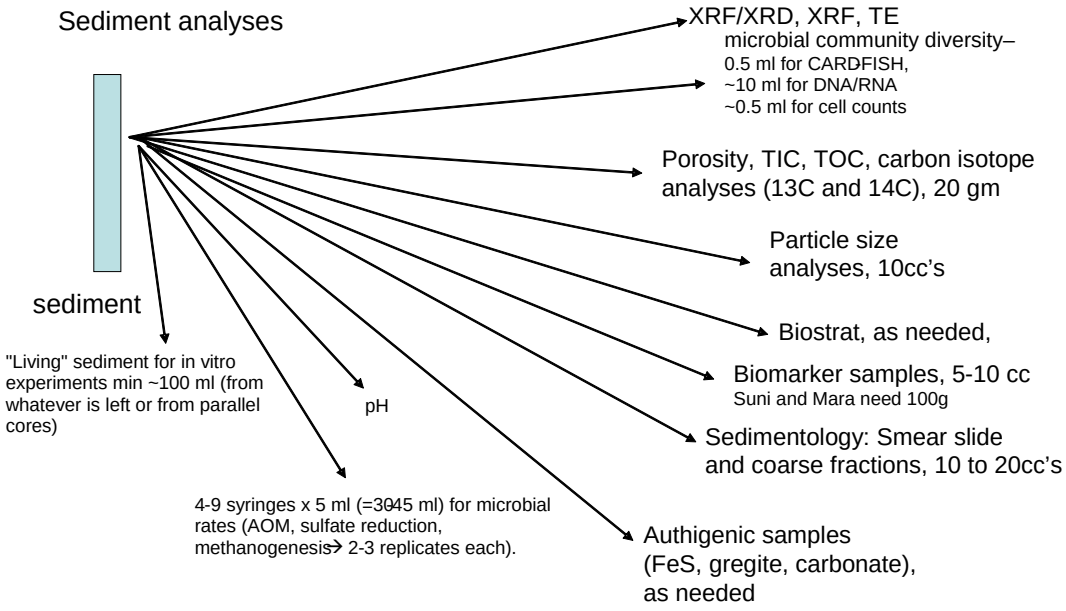

APPENDIX 7: Porewater data obtained at sea.

MITAS-2009-09
Porewater and Gas Data

Core	Syringe	Pore Water Sed Depth (cm)	Chloride (mM)	Sulfate (mM)	Sulfide (mM)	DIC (mM)	Gas Sample Sediment Depth (cm)	Gas Sample #	CH_4 (mM)	C_2H_6 (nM)	C_1/C_2 (vol)
VC01	1	15	nd	Nd	nd	nd	15	1	9.05E-04	0	
VC01	2	30	nd	Nd	nd	nd	30	2	7.88E-04	0	
VC01	3	45	nd	Nd	nd	nd	45	3	1.23E-03	0	
VC02	4	15	476.0	24.77	0.006	4.16	15	4	1.90E-04	0	
VC02	5	30	469.7	24.58	0.000	4.06	30	5	1.22E-04	0	
VC02	6	45	481.4	23.57	0.000	8.16	45	6	2.31E-04	0	
VC02	7	60	486.8	23.04	0.000	11.48	60	7	9.05E-04	0	
VC02	8	75	503.4	23.71	0.000	12.29	75	8	8.25E-04	0	
VC02	9	90	485.5	22.72	0.000	11.44	90	9	6.02E-04	0	
VC02	10	105	483.8	22.51	0.000	10.50	105	10	7.80E-04	0	
VC03	11	25	485.6	24.40	0.000	5.05	25	11	3.78E-04	0	
VC03	12	50	484.9	23.34	0.000	7.30	50	12	2.87E-04	0	
VC03	13	75	488.4	23.66	0.000	6.54	75	13	3.50E-04	0	
VC03	14	100	487.2	23.11	0.004	7.07	100	14	3.78E-04	0	
VC03	15	125	486.2	22.28	0.000	7.56	125	15	4.21E-04	0	
VC03	16	150	476.8	21.20	0.002	7.32	150	16	3.49E-04	0	
VC03	17	175	483.4	20.91	0.000	8.05	175	17	2.48E-04	0	
VC03	18	200	477.6	19.99	0.001	nd	200	18	1.45E-04	0	
VC03	19	225	463.7	19.43	nd	8.54	225	19	2.31E-04	0	
VC03	20	255	484.2	19.98	nd	7.14	255	20	2.53E-04	0	
PC02	21	661	533.7	26.28	0.005	4.92	661	21	1.19E-03	0	
PC02	22	641	539.2	26.40	0.002	5.15	641	22	8.90E-04	0	
PC02	23	621	533.6	26.01	0.001	5.52	621	23	9.71E-04	0	
PC02	24	601	533.3	25.73	0.000	5.75	601	24	8.72E-04	0	
PC02	25	571	541.3	25.98	0.000	6.39	571	25	6.91E-04	0	
PC02	26	541	538.2	25.71	0.000	7.29	541	26	8.09E-04	0	
PC02	27	511	547.7	26.02	0.000	6.81	511	27	9.00E-04	0	
PC02	28	471	549.4	25.84	0.000	7.53	471	28	7.91E-04	0	
PC02	29	441	542.1	25.56	0.000	7.77	441	29	7.10E-04	0	
PC02	30	401	537.5	25.26	0.000	8.08	401	30	6.76E-04	0	
PC02	31	365	542.4	25.51	0.000	8.08	365	31	7.35E-04	0	
PC02	32	325	551.1	26.00	0.002	8.15	325	32	7.14E-04	0	
PC02	33	285	554.0	26.56	0.002	7.31	285	33	5.20E-04	0	
PC02	34	245	551.0	26.70	0.002	6.87	245	34	5.17E-04	0	
PC02	35	205	543.0	25.84	0.000	6.87	205	35	4.61E-04	0	
PC02	36	165	554.3	27.39	0.000	6.50	165	36	3.28E-04	0	
PC02	37	125	552.2	27.52	0.003	6.22	125	37	2.95E-04	0	
PC02	38	95	547.4	27.61	0.000	5.86	95	38	1.17E-04	0	
PC02	39	60	545.5	27.89	0.003	5.21	60	39	1.54E-04	0	
PC02	40	30	534.4	27.86	0.002	4.05	30	40	1.87E-04	0	
PC03	41	675	505.5	19.57	0.010	7.18	675	41	8.24E-04	0	

PC03	42	645	501.8	19.52	0.003	7.61	645	42	1.10E-03	0	
PC03	43	625	498.1	19.55	0.002	7.87	625	43	8.85E-04	0	
PC03	44	610	499.5	19.58	0.004	7.90	610	44	1.06E-03	0	
PC03	45	585	507.8	19.98	0.000	8.27	585	45	1.28E-03	0	
PC03	46	555	509.1	20.12	0.003	8.60	555	46	1.19E-03	0	
PC03	47	525	509.2	20.40	0.001	8.91	525	47	1.06E-03	0	
PC03	48	485	512.9	20.94	0.003	9.23	485	48	1.16E-03	0	
PC03	49	455	500.8	20.68	0.002	9.28	455	49	8.32E-04	0	
PC03	50	420	504.0	21.29	0.000	10.16	420	50	7.54E-04	0	
PC03	51	370	501.4	21.63	0.002	9.95	370	51	8.19E-04	0	
PC03	52	330	509.4	22.36	0.002	8.70	330	52	1.65E-03	0	
PC03	53	280	511.2	23.26	0.002	8.29	280	53	7.27E-04	0	
PC03	54	240	509.5	23.51	0.003	7.77	240	54	6.65E-04	0	
PC03	55	200	503.2	23.43	0.001	7.56	200	55	6.14E-04	0	
PC03	56	160	507.3	24.22	0.000	7.26	160	56	1.05E-03	0	
PC03	57	120	493.8	23.98	0.004	7.09	120	57	4.07E-04	0	
PC03	58	60	507.9	25.37	0.000	5.93	60	58	4.37E-04	0	
PC03	59	20	503.4	26.23	0.000	4.76	20	59	2.94E-04	0	
PC04	60	369	497.3	21.10	0.010	5.67	369	60	1.07E-02	0	
PC04	61	344	506.7	24.33	0.007	4.45	344	61	4.74E-03	205.0	23
PC04	62	324	504.0	25.31	0.008	3.74	324	62	2.61E-03	0.0	
PC04	63	304	458.1	22.90	0.024	4.31	304	63	2.40E-03	0.0	
PC04	64	274	477.4	23.02	0.017	4.12	274	64	2.32E-03	0.0	
PC04	65	254	457.4	23.02	0.009	nd	254	65	1.93E-03	0.0	
PC04	66	234	460.0	23.34	0.028	2.53	234	66	1.92E-03	0.0	
PC04	67	214	464.1	23.58	0.014	3.74	214	67	1.92E-03	0.0	
PC04	68	194	453.5	22.89	0.014	3.64	194	68	1.48E-03	0.0	
PC04	69	164	458.9	22.35	0.013	5.06	164	69	1.38E-03	0.0	
PC04	70	144	453.6	23.19	0.010	3.67	144	70	1.28E-03	0.0	
PC04	71	124	467.7	23.73	0.013	3.21	124	71	1.20E-03	0.0	
PC04	72	99	466.3	23.66	0.018	3.65	99	72	1.12E-03	0.0	
PC04	73	70	472.0	24.28	0.010	3.44	70	73	8.88E-04	0.0	
PC04	74	50	466.5	24.18	0.015	3.60	50	74	8.36E-04	0.0	
PC04	75	30	465.6	24.15	0.008	3.70	30	75	2.51E-04	0.0	
PC04	76	10	464.4	24.55	0.015	3.66	10	76	8.37E-05	0.0	
PC06	77	301	531.6	23.17	nd	nd	301	77	1.92E-04	0.0	
PC06	78	286	578.2	25.63	0.000	nd	286	78	1.58E-04	0.0	
PC06	79	266	553.4	25.23	nd	nd	266	79	3.01E-04	0.0	
PC06	80	236	553.2	26.04	nd	nd	236	80	2.15E-04	0.0	
PC06	81	219			0.000	nd	219	81	1.51E-04	0.0	
PC06	82	196	568.1		nd	nd	196	82	1.50E-04	0.0	
PC06	83	176			nd	nd	176	83	1.66E-04	0.0	
PC06	84	156	524.7	25.59	nd	nd	156	84	1.95E-04	0.0	
PC06	85	136	525.1	26.04	nd	nd	136	85	1.44E-04	0.0	
PC06	86	116			nd	nd	116	86	1.49E-04	0.0	
PC06	87	96			nd	nd	96	87	1.68E-04	0.0	
PC06	88	76	533.9	27.0	nd	nd	76	88	1.62E-04	0.0	
PC06	89	61			nd	nd	61	89	1.75E-04	0.0	
PC06	90	35	504.4	26.47	0.002	3.59	35	90	1.30E-04	0.0	
PC06	91	13	511.9	26.54	0.001	3.67	13	91	8.28E-05	0.0	

PC07	92	140	509.6	23.68	0.005	4.64	140	92	5.88E-04	0.0	
PC07	93	120	527.6	25.12	nd		120	93	5.41E-04	0.0	
PC07	94	90	515.0	25.13	0.006	3.96	90	94	3.82E-04	0.0	
PC07	95	70	523.5	25.95	0.000	3.62	70	95	2.74E-04	0.0	
PC07	96	50	517.2	26.11	0.001	3.32	50	96	2.66E-04	0.0	
PC07	97	30	520.9	26.85	0.004	3.18	30	97	2.08E-04	0.0	
PC07	98	13	515.7	27.13	0.003	2.90	13	98	1.27E-04	0.0	
PC08	99	215	477.4	0.46	0.007	15.34	215	99	4.02E+00	104.4	38496
PC08	100	195	481.8	0.40	0.006	17.27	195	100	3.27E+00	152.5	21455
PC08	101	180	482.5	0.51	0.008	18.21	180	101	1.70E+00	161.8	10536
PC08	102	160	486.9	2.62	0.005	19.81	160	102	1.26E-01	117.2	1074
PC08	103	145	487.5	5.21	0.008	17.84	145	103	7.76E-02	100.0	776
PC08	104	130	486.7	7.60	0.004	16.44	130	104	4.20E-02	82.0	512
PC08	105	110	505.6	11.38	0.003	14.18	110	105	2.34E-02	69.2	338
PC08	106	90	495.4	15.58	0.004	10.98	90	106	5.09E-03	22.5	226
PC08	107	70	496.2	19.22	0.003	7.63	70	107	3.73E-03	0.0	
PC08	108	50	496.5	22.00	0.004	6.30	50	108	2.23E-03	0.0	
PC08	109	30	497.9	25.03	0.004	4.00	30	109	1.34E-03	0.0	
PC08	110	13	483.8	25.51	0.008	2.71	13	110	6.37E-04	0.0	
PC09	111	392	517.4	1.19	0.000	47.41	392	111	1.97E-03	0.0	
PC09	112	372	512.2	1.60	0.000	45.62	372	112	2.20E-03	0.0	
PC09	113	352	518.1	2.11	0.000	44.20	352	113	2.68E-03	0.0	
PC09	114	322	524.1	3.05	0.000	44.43	322	114	3.04E-03	0.0	
PC09	115	292	522.2	4.13	0.014	42.85	292	115	3.13E-03	0.0	
PC09	116	262	513.2	5.25	0.012	40.29	262	116	3.24E-03	0.0	
PC09	117	232	521.5	6.81	0.009	38.43	232	117	3.03E-03	0.0	
PC09	118	202	522.5	8.15	0.003	36.18	202	118	3.06E-03	0.0	
PC09	119	172	525.4	10.25	0.009	25.67	172	119	2.85E-03	0.0	
PC09	120	137	522.0	12.25	0.006	27.86	137	120	2.66E-03	0.0	
PC09	121	90	525.0	17.32	0.012	18.92	90	121	1.77E-03	0.0	
PC09	122	60	527.4	21.65	0.020	12.81	60	122	1.32E-03	0.0	
PC09	123	20	523.7	25.69	0.006	7.03	20	123	7.21E-04	0.0	
PC10	124	568	nd	Nd	nd	nd	568	124	4.81E-04	0.0	
PC10	125	548	nd	Nd	nd	nd	548	125	6.31E-04	0.0	
PC10	126	528	nd	Nd	nd	nd	528	126	4.77E-04	0.0	
PC10	127	508	nd	Nd	nd	nd	508	127	5.36E-04	0.0	
PC10	128	478	519.4	15.4	0.006	nd	478	128	4.76E-04	0.0	
PC10	129	448	518.4	15.0	0.029	16.40	448	129	6.22E-04	0.0	
PC10	130	418	516.5	17.0	0.020	12.16	418	130	5.64E-04	0.0	
PC10	131	378	520.6	18.0	0.003	12.41	378	131	6.48E-04	0.0	
PC10	132	348	517.0	18.6	0.006	12.25	348	132	7.04E-04	0.0	
PC10	133	323	522.1	19.4	0.006	11.43	323	133	7.08E-04	0.0	
PC10	134	301	525.0	20.2	0.020	11.61	301	134	6.63E-04	0.0	
PC10	135	270	515.9	20.6	0.012	10.44	270	135	5.69E-04	0	
PC10	136	230	528.7	21.9	0.014	10.52	230	136	5.52E-04	0	
PC10	137	190	527.0	22.7	0.009	9.06	190	137	4.93E-04	0	
PC10	138	150	527.6	23.7	0.009	8.15	150	138	4.58E-04	0	
PC10	139	110	526.1	24.8	0.023	7.01	110	139	4.16E-04	0	
PC10	140	70	525.8	25.9	0.012	5.86	70	140	2.93E-04	0.0	
PC10	141	20	524.3	27.4	0.014	4.78	20	141	1.58E-04	0.0	

PC11	142	546	518.6	9.1	0.000	25.57	546	142	1.00E-03	0.0	
PC11	143	526	518.7	9.1	0.003	26.44	526	143	1.16E-03	0.0	
PC11	144	506	517.1	9.1	0.000	26.58	506	144	1.30E-03	0.0	
PC11	145	486	510.6	9.1	0.003	26.41	486	145	1.61E-03	0.0	
PC11	146	456	517.5	9.5	0.003	26.36	456	146	1.63E-03	0.0	
PC11	147	426	507.1	9.6	0.009	26.50	426	147	1.60E-03	0.0	
PC11	148	396	519.6	10.2	0.006	26.39	396	148	1.33E-03	0.0	
PC11	149	356	521.9	11.1	0.023	25.99	356	149	1.51E-03	0.0	
PC11	150	326	520.5	12.0	0.003	24.53	326	150	1.54E-03	0.0	
PC11	151	296	521.6	13.2	0.012	22.86	296	151	1.66E-03	0.0	
PC11	152	250	520.6	15.2	0.006	20.00	250	152	1.50E-03	0.0	
PC11	153	210	520.5	16.3	0.009	18.64	210	153	1.32E-03	0.0	
PC11	154	170	526.3	18.4	0.003	16.42	170	154	1.12E-03	0.0	
PC11	155	130	520.8	20.1	0.017	12.43	130	155	8.59E-04	0.0	
PC11	156	90	518.3	22.4	0.023	9.56	90	156	6.98E-04	0.0	
PC11	157	50	rerun	Rerun	0.020	7.96	50	157	4.80E-04	0.0	
PC11	158	15	rerun	Rerun	0.012	5.62	15	158	2.63E-04	0.0	
PC12	159	585	rerun	Rerun	0.000	63.36	585	159	8.93E+00	851.191	10488
PC12	160	565	rerun	Rerun	0.000	60.23	565	160	1.10E+01	1049.16	10513
PC12	161	545	rerun	Rerun	0.000	64.68	545	161	1.03E+01	965.998	10615
PC12	162	525	rerun	Rerun	0.000	64.08	525	162	1.12E+01	997.565	11276
PC12	163	505	507.6	0.3	0.000	63.84	505	163	1.06E+01	927.226	11464
PC12	164	485	515.1	0.3	0.007	61.15	485	164	1.20E+01	1012.13	11850
PC12	165	465	519.7	0.3	0.000	63.18	465	165	1.26E+01	1068.1	11758
PC12	166	445	525.5	0.3	0.000	61.51	445	166	1.21E+01	916.0	13210
PC12	167	425	529.0	0.3	0.000	60.68	425	167	1.23E+01	901.973	13644
PC12	168	405	519.0	0.3	0.000	51.52	405	168	1.12E+01	699.177	15977
PC12	169	385	519.4	0.4	0.002	57.94	385	169	1.18E+01	713.875	16562
PC12	170	365	533.0	0.4	0.004		365	170	1.23E+01	722.642	17019
PC12	171	345	519.6	0.5	0.004	55.45	345	171	1.13E+01	553.794	20418
PC12	172	325	525.7	0.6	0.015	54.59	325	172	1.12E+01	537.205	20912
PC12	173	305	523.0	0.5	0.007	52.65	305	173	1.14E+01	537.747	21174
PC12	174	280	524.6	0.4	0.013	52.18	280	174	1.22E+01	526.971	23177
PC12	175	260	513.5	0.6	0.009	50.87	260	175	1.11E+01	405.405	27358
PC12	176	240	513.7	0.8	0.005	48.84	240	176	9.82E+00	280.538	35000
PC12	177	220	507.3	1.0	0.011	46.32	220	177	8.86E+00	253.803	34921
PC12	178	190	510.3	0.7	0.004	45.33	190	178	6.27E+00	177.319	35381
PC12	179	170	515.8	1.6	0.004	42.53	170	179	4.15E+00	255.108	16260
PC12	180	150	511.1	1.4	0.002	39.99	150	180	2.18E+00	81.4573	26709
PC12	181	130	516.6	2.5	0.002	38.55	130	181	1.74E-01	71.2553	2437
PC12	182	110	513.7	7.3	0.002	30.62	110	182	1.38E-02	51.1	269
PC12	183	88	510.6	12.0	0.004	23.60	88	183	1.25E-02	0	
PC12	184	70	519.9	18.3	0.000	15.90	70	184	9.66E-03	0.0	
PC12	185	50	502.4	23.6	0.000	7.50	50	185	6.40E-03	0	
PC12	186	20	509.6	26.1	0.000	4.74	20	186	3.47E-03	0	
PC13	187	551	nd	Nd	nd	nd	551	187	1.32E+01	86.3418	152671
PC13	188	546	494.5	0.4	0.000	79.39	546	188	1.04E+01	72.9966	142405
PC13	189	526	495.8	0.4	0.000	76.18	526	189	1.08E+01	50.4031	215089
PC13	190	506	504.2	0.4	0.011	70.05	506	190	1.09E+01	152.096	71972
PC13	191	486	490.0	0.4	0.004	71.92	486	191	1.10E+01	163.555	67083

PC13	192	466	492.4	0.4	0.007	68.16	466	192	1.42E+01	92.9787	153190
PC13	193	446	497.3	0.4	0.000	64.62	446	193	1.18E+01	46.4269	254552
PC13	194	426	490.1	0.4	0.004	67.69	426	194	1.16E+01	53.6139	215909
PC13	195	406	507.8	0.4	0.002	68.76	406	195	1.18E+01	50.3325	235208
PC13	196	386	501.8	0.4	0.000	66.55	386	196	1.20E+01	50.2407	238637
PC13	197	366	489.2	0.5	0.000	65.62	366	197	1.19E+01	49.6199	239556
PC13	198	346	489.3	0.6	0.002	62.64	346	198	1.23E+01	46.4137	264407
PC13	199	321	503.0	0.4	0.002	72.64	321	198	1.16E+01	40.0161	291098
PC13	200	280	504.8	0.5	0.007	59.51	280	198	1.24E+01	43.6654	283877
PC13	201	260	505.1	0.7	0.005	58.24	260	198	1.18E+01	44.5809	264088
PC13	202	240	502.0	0.6	0.000	58.54	240	198	1.16E+01	41.41	279121
PC13	203	210	505.3	0.5	0.007	57.22	210	198	1.08E+01	46.0156	234309
PC13	204	190	501.1	0.7	0.000	52.08	190	198	8.54E+00	38.5944	221290
PC13	205	170	501.9	0.6	0.000	50.89	170	198	8.96E+00	34.0458	263043
PC13	206	150	494.0	0.7	0.000	47.80	150	198	7.54E+00	33.6281	224203
PC13	207	130	490.2	0.6	0.000	45.60	130	198	4.13E+00	44.2363	93338
PC13	208	110	501.9	0.5	0.027	41.08	110	198	1.35E+00	67.409	19988
PC13	209	88	500.8	3.7	0.009	35.40	88	198	1.28E-01	21.6598	5888
PC13	210	70	504.7	9.8	0.016	26.69	70	198	2.71E-02	0.0	
PC13	211	50	508.3	16.8	0.005	17.83	50	198	1.11E-02	0.0	
PC13	212	15	508.9	26.7	0.005	3.68	15	198	2.94E-03	0.0	
PC14	213	613			0.000	54.53	613	213	4.11E+00	0	
PC14	214	593	510.7	0.4	0.002	54.71	593	214	3.35E+00	0	
PC14	215	573			0.000	54.18	573	215	2.79E+00	17.7395	157491
PC14	216	553	510.2	0.5	0.000	54.79	553	216	2.57E+00	0	
PC14	217	523			0.000	53.22	523	217	2.14E+00	0	
PC14	218	483	516.7	0.5	0.000	50.24	483	218	1.48E+00	0	
PC14	219	453			0.000	51.64	453	219	9.68E-01	0	
PC14	220	413	506.0	0.6	0.000	52.04	413	220	3.68E-01	0	
PC14	221	373			0.000	49.46	373	221	2.03E-01	0	
PC14	222	328	506.3	2.7	0.000	46.41	328	222	1.21E-01	0	
PC14	223	288			0.033	43.07	288	223	7.24E-02	0	
PC14	224	248	507.3	6.2	0.000	38.37	248	224	4.45E-02	0.0	
PC14	225	208			0.000	35.10	208	225	2.80E-02	0.0	
PC14	226	168	505.2	11.6	0.000	28.03	168	226	2.10E-02	0.0	
PC14	227	128			0.000	20.81	128	227	1.13E-02	0.0	
PC14	228	98	505.0	17.4	0.000	18.86	98	228	7.43E-03	0	
PC14	229	58			0.000	13.28	58	229	4.19E-03	0	
PC14	230	18	510.1	25.3	0.000	6.12	18	230	1.80E-03	0	